PHYSICAL REVIEW B VOLUME 46, NUMBER 10 1 SEPTEMBER 1992-II

Site-selective laser spectroscopy of Pr^{3+} C_{4v} symmetry centers in hydrogenated CaF_2:Pr^{3+} and SrF_2:Pr^{3+} crystals

R. J. Reeves,* G. D. Jones, and R. W. G. Syme

Department of Physics, University of Canterbury, Christchurch, New Zealand

(Received 1 July 1991; revised manuscript received 26 May 1992)

Laser-selective excitation and optical-absorption techniques have been used to establish comprehensive sets of energy levels for both the F^- and hydrogenic varieties of the tetragonal symmetry (C_{4v}) centers in SrF_2 and CaF_2. Polarization of the various spectral lines was used to determine the symmetry labels of many of the energy levels. Reversals of the ordering of some levels between SrF_2 and CaF_2 are found and, in particular, the two lowest levels (D_1 and D_2) of the $^1D_2$ multiplet, which are the originating levels for many of the observed emission transitions, have reversed-symmetry label assignments in SrF_2 and CaF_2. Differences were found between the ground-state Zeeman splittings for the C_{4v} F^- and D^- centers for both SrF_2 and CaF_2. Fluorescence lifetimes of the C_{4v} hydrogenic centers show a strong dependence on the particular charge-compensating ion present through nonradiative decay processes involving the respective local mode phonons. The upconversion spectra observed for F^-, T^-, and D^- varieties of the C_{4v} centers in SrF_2 and for the C_{4v} F^- center in CaF_2 are all consistent with excitation of specific subsets of nearby C_{4v} centers.

I. INTRODUCTION

Laser-selective excitation (LSE) is a powerful method for resolving lines of multicenter spectra and has been used with good success in the characterization of many hydrogenic centers in CaF_2:Er^{3+} crystals.[1] In this technique a tunable dye laser is used selectively to excite a particular absorption transition of a given center and the resulting fluorescence is monitored. If the absorption line pumped is sufficiently well isolated from others, only the selected center is excited and the resulting fluorescence arises from this center alone.

The CaF_2:Pr^{3+} system has been extensively studied and both single Pr^{3+} ion and Pr^{3+} cluster centers identified.[2] Because cross relaxation in the multi-Pr^{3+} cluster centers strongly quenches Pr^{3+} emission from the $^1D_2$ multiplet, monitoring of up-conversion fluorescence from the higher energy $^3P_0$ multiplet has been used to characterize such centers.[3]

The principal Pr^{3+} absorbing species in both CaF_2:0.05% Pr^{3+} and SrF_2:0.05% Pr^{3+} crystals is the well-established tetragonal (C_{4v}) symmetry center in which the charge compensating F^- ion is in the nearest interstitial position, i.e., in a [100] direction from the Pr^{3+} ion. We present here the detailed results of a LSE study of such C_{4v} symmetry centers in these crystals both before and after hydrogenation. Preliminary results have been given in an earlier brief account,[4] while the spectroscopy of the multihydrogenic centers, which exhibit polarized bleaching, has already been reported.[5]

An extensive investigation of the C_{4v} F^- center in SrF_2:Pr^{3+}, detailed in Sec. III B, has identified the energies and symmetry labels of 49 of the possible 70 levels of the $4f^2$ configuration for Pr^{3+} ions in C_{4v} symmetry centers. A similar study of the corresponding center in CaF_2:Pr^{3+} is given in Sec. III C. However, as the symmetry labels of the two lowest energy levels, D_1 and D_2, of the $^1D_2$ multiplet are interchanged in CaF_2 as compared to SrF_2, fewer fluorescent transitions are observed and the spectroscopy of the CaF_2 C_{4v} F^- center is less complete. Of the 70 possible levels, the energies and symmetry labels of 34 have been determined. The fluorescence of the analogous C_{4v} hydrogenic centers is much weaker,[6] and discrimination of their features from those of the much stronger emitting F^- centers and from lines attributed to traces of Sm^{2+} and Nd^{3+} impurities in the crystals requires careful choice of laser excitation energies. Nevertheless, a total of 36 and 32 transitions are unambiguously identified for these centers in deuterated SrF_2:Pr^{3+} and CaF_2:Pr^{3+} respectively.

II. EXPERIMENTAL TECHNIQUES

For all the spectroscopic measurements, calcium and strontium fluoride crystals containing, unless otherwise indicated, 0.05% molar concentration of praseodymium were either purchased from Optovac, Inc., or grown in this institution from the melt by the Bridgman-Stockbarger technique. For the locally grown samples, appropriate amounts of the alkaline earth fluoride and PrF_3 were placed in a graphite crucible and lowered through the temperature gradient produced by the heating coil of a 38 kW Arthur D. Little R.F. furnace at a lowering rate of 4 mm/h. Oriented crystals for polarization studies were cut from boules aligned using the {111} cleavage planes.

Hydrogen or deuterium was introduced[7] by heating the crystals in contact with molten aluminum in the appropriate hydrogen isotope atmosphere (at 250 mm of mercury pressure) to 850 °C for periods ranging from 24 to 68 h. Various cooling rates after hydrogenation were used depending on site distributions required, and these

©1992 The American Physical Society

rates ranged from a gradual cool down to room temperature over several hours to immediate immersion of the quartz hydrogenation tube in liquid nitrogen.

The preparation of the tritiated samples necessitated a more compact, sealed system enclosing the glass ampoule which contained the tritium gas. Even with this arrangement, the attainable tritium gas pressure was only about one tenth of that possible in the normal hydrogenation and deuteration arrangement.

Optical absorption spectra showing transitions to levels of the ${}^1G_4$, ${}^1D_2$, ${}^3P_0$, and ${}^3P_1$ multiplets of the Pr^{3+} ion were recorded photoelectrically on a Spex 1700 0.75 m monochromator using an EMI 9558QA or RCA 7102 photomultiplier as appropriate. Source radiation was from a voltage-stabilized 100-W quartz iodine lamp. Spectra were recorded at temperatures down to 10 K using a Cryosystem LTS22.1 closed-cycle conduction-type cryostat.

A Spectra Physics 375 dye laser pumped by a Spectra Physics 171 argon ion laser was used for the laser excitation and a Spex 1403 double monochromator equipped with a thermoelectrically cooled RCA 31034A photomultiplier recorded the fluorescence spectra under computer control. Photon counting techniques were used to give the high sensitivity needed to detect weak fluorescence lines. Rhodamine 590 dye was appropriate for laser excitation of the electronic levels of the ${}^1D_2$ multiplet of praseodymium with the laser power being typically 100 mW. A birefringent tuning element in the dye laser gave a spectral linewidth of 1 cm^{-1} and allowed continuous tuning of the laser through the fluorescence range of the dye.

Local mode vibronic energy levels, in the 18 000 cm^{-1} spectral region associated with the ${}^1D_2$ multiplet, were excited using a coumarin 540 dye pumped with the 488.0 nm argon laser line, for a typical output power of 15 mW. Fluorescence from the ${}^1D_2$ multiplet to the energy levels of the ${}^3F_2$, ${}^3F_3$, and ${}^3F_4$ multiplets in the region below 11 600 cm^{-1} was analyzed by a Spex 1700 monochromator equipped with an RCA 7102 photomultiplier tube cooled to −100 °C in a Products for Research model TE-176-RF liquid-nitrogen refrigeration chamber. The output signal was recorded on a Keithley 180B electrometer.

Polarization spectra were recorded using a Spectra Physics model 310 polarization rotator to determine the laser polarization direction, and a polaroid sheet as an analyzer. For the infrared fluorescence studies, an infrared HRB polaroid sheet was used. A polarization scrambler equalized the spectrometer response for different polarizations.

All reported wave numbers are as measured in air. Fluorescent lifetimes were measured using a Photochemical Research Associates (PRA) model LN107 dye laser pumped by a PRA LN1000 pulsed nitrogen laser. The dye laser has an output of up to 100 μJ per pulse, and a bandwidth of typically 0.04 nm. Rhodamine 590 and Coumarin 481 were appropriate for the excitation of the ${}^1D_2$ and ${}^3P_0$ multiplets, respectively. The emission was analyzed using the Spex 1700 monochromator equipped with an RCA C31034 photomultiplier thermoelectrically cooled to −25 °C. Signal output from a preamplifier stage was processed by a Stanford Research Systems model SRS250 boxcar system, triggered by a signal produced by a pyroelectric detector monitoring the laser beam.

Measurements of the Pr^{3+} $({}^3H_4,\Gamma_5^+,\gamma_5)$ ground-state g values were made using a six-telsa Oxford Instruments superconducting magnet at the IBM Almaden Center. The magnetic-field-induced splitting of this orbitally degenerate ground state was monitored by fluorescence excitation using a single mode Coherent 599 dye laser as the excitation source.

III. SPECTROSCOPY OF Pr^{3+} IN THE ALKALINE EARTH FLUORIDES BEFORE HYDROGENATION

The principal spectral features of both CaF_2:0.05% Pr^{3+} and SrF_2:0.05% Pr^{3+} originate from a single Pr^{3+} ion in the C_{4v} symmetry center. Direct evidence of the positioning of the charge-compensating F^- ion in the nearest interstitial position has been provided by high resolution laser studies.[8,9] Absorption and emission measurements[10] previously identified some of the energy levels of the C_{4v} centers in both $CaF_2:Pr^{3+}$ and $SrF_2:Pr^{3+}$. While this C_{4v} F^- center is predominant in $SrF_2:Pr^{3+}$, other centers appear at comparable intensity in $CaF_2:Pr^{3+}$. As these other centers have been extensively studied,[2] they were not investigated further in this work.

A. Energy levels of the C_{4v} symmetry centers

The $4f^2$ configuration, appropriate for trivalent Pr^{3+} ions, has a total of 91 electronic states. There are 70 distinct energy levels for Pr^{3+} ions located in sites of C_{4v} symmetry, and each of the corresponding wave functions necessarily transforms as one of the irreps (γ) of the C_{4v} point group. As the C_{4v} Pr^{3+} symmetry can be regarded as a perturbation of the cubic symmetry of a Pr^{3+} ion located in an immediate environment of eight F^- ions, the various irreps Γ^+ of the octahedral (O_h) group can be used to distinguish between levels having the same C_{4v} symmetry label. Repeated O_h irreps of a given ${}^{2S+1}L_J$ multiplet are distinguished by primes. The complete nomenclature for labeling the various Pr^{3+} levels in the C_{4v} centers includes, therefore, the parent ${}^{2S+1}L_J$ multiplet and their symmetry labels, Γ^+ and γ for the O_h and C_{4v} point groups, respectively. In this notation, the ground state is the $({}^3H_4,\Gamma_5^+,\gamma_5)$ doublet and the single level of the ${}^3P_0$ multiplet is the $({}^3P_0,\Gamma_1^+,\gamma_1)$ state.

In the cases where the symmetry label of a particular level is not known or need not be specified, a notation of a letter plus numerical label is adopted for labeling crystal-field levels of the various ${}^{2S+1}L_J$ multiplets. The ground multiplet is labeled Z, with the ground state being Z_1, and the first excited multiplet by Y. For Pr^{3+} ions, the levels of the ${}^1D_2$ multiplet are arbitrarily labeled D_1, D_2, D_3, and D_4, in order of increasing energy. The electric-dipole transitions for C_{4v} site symmetry can be characterized as either σ or π, corresponding to the **E** vector of the light being respectively perpendicular or parallel to the four-fold axis (C_4) of the C_{4v} site. For a given C_{4v} center, electric-dipole transitions are not allowed between some levels. The absence of such transitions from the spectrum leads to gaps in the energy level scheme and care is needed to assign energy levels correctly.

Polarization of the LSE spectra can help in assigning symmetry labels to levels. At first appearance no polarization effects might be expected for C_{4v} symmetry centers in the CaF_2 structure because of the three possible orientations of the principal axis of symmetry. However, some orientations of these centers are preferentially excited by polarized laser light incident along a crystal symmetry direction, giving a net polarized emission. Table I gives the electric-dipole selection rules for even-electron ions, such as Pr^{3+}, and the relative polarization intensities for tetragonal symmetry (C_{4v}) centers in $\langle 100 \rangle$ oriented crystals. In this table, the polarization geometry for $\langle 100 \rangle$ oriented crystals is specified by $x(ab)z$, where x is the direction of the incident laser beam, z is the direction of propagation of the fluorescence, and a, b are the polarization directions of the laser light and fluorescence, orthogonal to x and z respectively. For C_{4v} centers in CaF_2 type crystals, the orientation of the C_4 axis is determined by the position of the charge-compensating ion. Polarization effects occur because the particular C_{4v} centers with their C_4 axes oriented either in the direction of propagation of the laser beam or in the direction of propagation of the collected fluorescence cannot respectively absorb or emit π-polarized radiation. Also indicated in Table I are the corresponding relative polarization intensities for a magnetic-dipole decay transition, σ' or π', as determined by the **B** vector alignment.

The electric-dipole polarization intensity ratios for $\langle 111 \rangle$ crystal orientation have been presented for the case of odd electrons.[1] Table II gives the corresponding results for even-electron ions, such as Pr^{3+}. As for the previous case of odd electrons, the polarization is specified using primed axes, with the z' axis in a crystal [111] direction. The various polarizations are labeled by $x'(a'b')z'$, where x' is the direction of the incident laser beam in the selected (111) plane, z' is the direction of propagation of the fluorescence, and a',b' are the polarization directions of the laser light and fluorescence, orthogonal to x' and z' respectively.

All the fluorescence transitions observed here for Pr^{3+} in sites of C_{4v} symmetry are from singlet levels (γ_1 or γ_3) of the $^1D_2$ or $^3P_0$ multiplets which are excited only by σ-

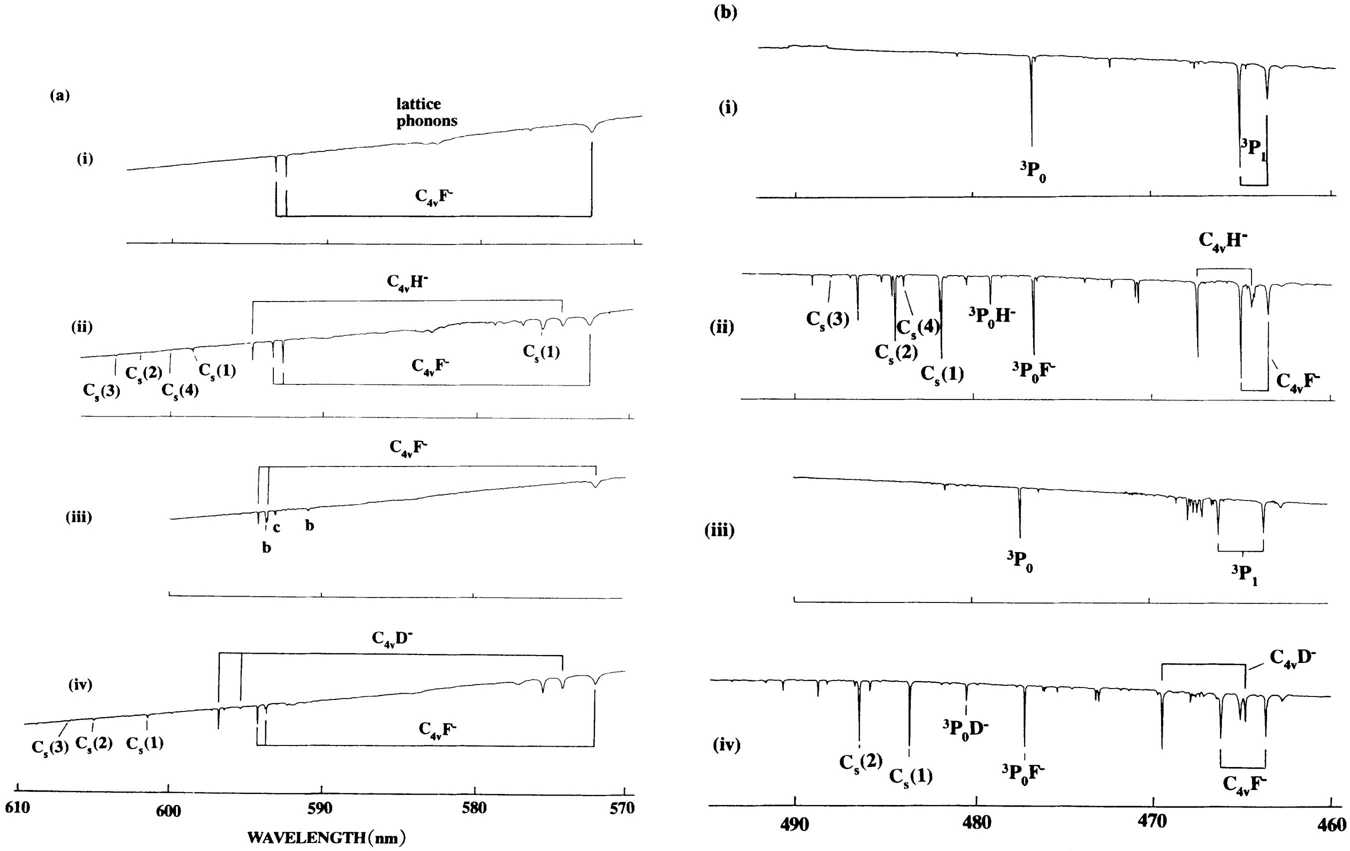

FIG. 1. 14 K optical transmission spectra for (i) $SrF_2:Pr^{3+}$; (ii) hydrogenated $SrF_2:Pr^{3+}$; (iii) CaF_2:0.02% Pr^{3+}; and, (iv) deuterated $CaF_2:Pr^{3+}$. Transitions to energy levels of (a) the $^1D_2$ and (b) the $^3P_0$ and $^3P_1$ multiplets of the C_{4v} centers are identified. The lines marked by "b" or "c" arise from other centers present in $CaF_2:Pr^{3+}$ before deuteration, while the lines labeled $C_s(1)$, $C_s(2)$, $C_s(3)$, or $C_s(4)$ identify bleacheable hydrogenic centers. Zero transmission has been suppressed to show weak features.

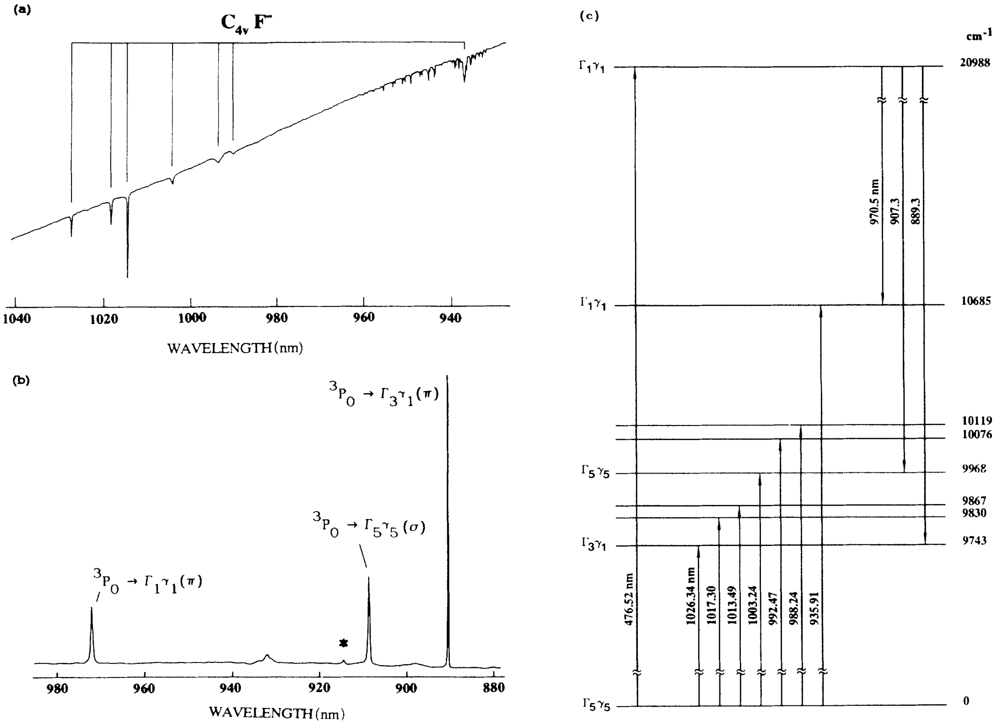

FIG. 2. (a) 14 K $^1G_4$ multiplet transmission spectrum (with zero transmission suppressed), (b) 14 K fluorescence spectrum of $^3P_0$ to $^1G_4$ multiplet transitions (* identifies the $R_1 \rightarrow Z_5$ transition of Nd^{3+}), and (c) the $^1G_4$ multiplet energy level scheme showing transitions (in nm) observed to and from energy levels (cm^{-1} in air) of the $^1G_4$ multiplet for the C_{4v} F^- center in SrF_2:Pr^{3+} crystals. Wavelength uncertainties are ±0.02 nm, and energy uncertainties are ± 1 cm^{-1}.

polarized absorption transitions from the $^3H_4$ ground doublet level (γ_5 symmetry). The allowed electric-dipole fluorescence transitions are either to singlet levels of γ_1 or γ_3 symmetry or to doublet levels of γ_5 symmetry giving the relative polarization intensities summarized in Table I. The markedly different polarization ratios unequivocally distinguish a singlet (here γ_1 or γ_3) terminating level from a doublet (γ_5) terminating level.

The comprehensive set of energy levels obtained for the C_{4v} F^- centers is sufficiently complete for a crystal-field analysis to obtain accurate crystal-field wave functions needed for the calculation of (X,Y) local-mode vibronic splittings. Details of such crystal-field and vibronic splitting calculations and their comparison with experimental observations will be presented elsewhere.

The spectroscopy of the C_{4v} centers is now discussed in turn for SrF_2:Pr^{3+} and CaF_2:Pr^{3+}.

B. The C_{4v} F^- center in SrF_2:Pr^{3+}

The absorption transitions of the Pr^{3+} ion in the C_{4v} F^- center are indicated in Figs. 1 and 2. Transitions to the $^3P_0$ and $^3P_1$ multiplets have previously been identified,[10] but this is the first identification of the transitions to the $^1G_4$ levels. Other absorbing centers, which are clearly present in the $^3P_0$ absorption spectrum, are not discussed further here as their spectroscopy has already been documented.[5]

Absorption transitions to three of the four crystal-field levels of the $^1D_2$ multiplet have been identified. Assignment of the D_4 crystal-field level was subsequently confirmed by laser excitation results (Fig. 3). The position of the missing D_3 component could not be determined in the absorption spectrum.

Six of the several absorption transitions to the crystal-field levels of the $^1G_4$ multiplet appear in the 7900–10120 cm^{-1} region. The seventh was located at 10 685 cm^{-1} amidst fine-line structure in the emission from the quartz iodine light source (Fig. 2). Estimates of the crystal field confirmed this large overall splitting for the $^1G_4$ multiplet and identified the level at 10 685 cm^{-1} as the (Γ_1^+,γ_1) state of $^1G_4$.

Absorption transitions identified for the C_{4v} F^- center are summarized in Table III.

An interesting feature of the absorption results is the near coincidence of the absorption transition to the $^3P_0$ multiplet at 476.52 nm (20 985.4 cm^{-1}) with the blue 476.5 nm line of the argon ion laser. A similar coincidence occurs between the corresponding transition of the $C_s(3)$ center[5] and the 488.0 nm argon laser line. These coincidences were used to excite Pr^{3+} ions in these centers for the recording of their $^3P_0$ emission.

The Pr^{3+} ion in the C_{4v} F^- center is known to exhibit hole burning with hyperfine and superhyperfine structure visible for some transitions.[8,9] In principle, such high resolution studies could be repeated for those centers exhibiting a near coincidence by Zeeman sweeping the transitions through a single-mode argon laser line. Using the

TABLE I. Relative polarization intensities for tetragonal (C_{4v}) centers in ⟨100⟩-oriented crystals. $\gamma_a=\gamma_1, \gamma_2, \gamma_3, \gamma_4$ or γ_5; $\gamma_{a'}=\gamma_1, \gamma_2, \gamma_3$ or γ_4.

Pump transition	Decay transition		Polarization geometry $x(yy)z$	$x(yx)z$	$x\left(\begin{smallmatrix}zx\\ zy\end{smallmatrix}\right)z$
Electric dipole	Electric dipole				
$\gamma_a\rightarrow\gamma_a(\pi)$	$\gamma_a\rightarrow\gamma_a$	(π)	1	0	0
	$\gamma_{a'}\leftrightarrow\gamma_5$	(σ)	0	1	1
$\gamma_{a'}\leftrightarrow\gamma_5(\sigma)$	$\gamma_a\rightarrow\gamma_a$	(π)	0	1	1
	$\gamma_{a'}\leftrightarrow\gamma_5$	(σ)	2	1	1
	Magnetic dipole				
$\gamma_a\rightarrow\gamma_a(\pi)$	$\gamma_1\leftrightarrow\gamma_2$ $\gamma_3\leftrightarrow\gamma_4$ $\gamma_5\rightarrow\gamma_5$	(π')	0	1	0
	$\gamma_{a'}\leftrightarrow\gamma_5$	(σ')	1	0	1
$\gamma_{a'}\leftrightarrow\gamma_5(\sigma)$	$\gamma_1\leftrightarrow\gamma_2$ $\gamma_3\leftrightarrow\gamma_4$ $\gamma_5\rightarrow\gamma_5$	(π')	1	0	1
	$\gamma_{a'}\leftrightarrow\gamma_5$	(σ')	1	2	1

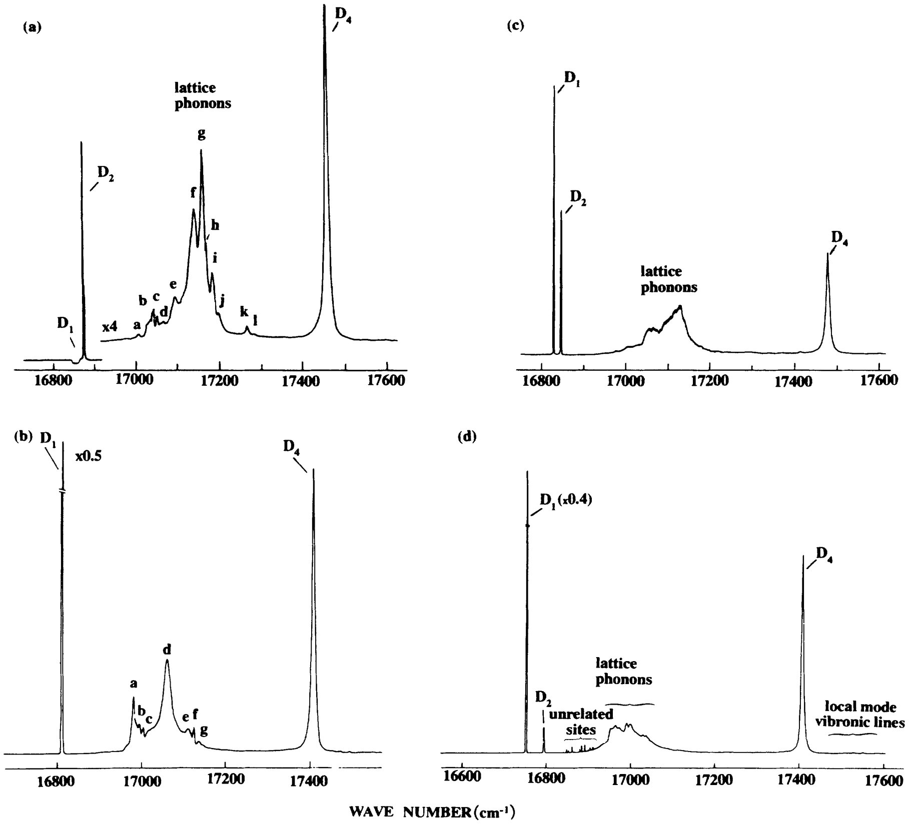

FIG. 3. 14 K excitation spectra of the ${}^1D_2$ multiplet obtained by monitoring D_1 to Z_1 fluorescence [in (a)] or D_1 to Z fluorescence near 625 nm: (a) the C_{4v} F^- center in SrF_2:Pr^{3+} (the lattice phonon lines marked "*a*" to "*l*" are listed in Table IV); (b) the C_{4v} D^- center in deuterated SrF_2:Pr^{3+} (the lattice phonon lines marked "*a*" to "*g*" are listed in Table IV); (c) the C_{4v} F^- center in CaF_2:Pr^{3+}; and (d) the C_{4v} D^- center in deuterated CaF_2:Pr^{3+}. Absorption transitions to the energy levels of the ${}^1D_2$ multiplet are identified by D_1, D_2, or D_4.

TABLE II. Predicted electric dipole polarization intensity ratios for tetragonal (C_{4v}) and trigonal (C_{3v}) centers in a $\langle 111 \rangle$-oriented crystal.

		Polarization ratios	
Pump transition	Decay transition	$\frac{x'(y'y')z'}{x'(y'x')z'}$	$\frac{x'(y'x')z'}{x'(z'x')z'}$
C_{4v} centers ($\gamma_a = \gamma_1, \gamma_2, \gamma_3, \gamma_4$, or γ_5; $\gamma_{a'} = \gamma_1, \gamma_2, \gamma_3$, or γ_4)			
$\gamma_a \rightarrow \gamma_a$	$\gamma_a \rightarrow \gamma_a$	3	$\frac{1}{2}$
	$\gamma_{a'} \leftrightarrow \gamma_5$	$\frac{3}{5}$	$\frac{5}{4}$
$\gamma_{a'} \leftrightarrow \gamma_5$	$\gamma_a \rightarrow \gamma_a$	$\frac{3}{5}$	$\frac{5}{4}$
	$\gamma_{a'} \leftrightarrow \gamma_5$	$\frac{9}{7}$	$\frac{7}{8}$
C_{3v} centers ($\gamma_a = \gamma_1$ or γ_2)			
$\gamma_a \rightarrow \gamma_a$	$\gamma_a \rightarrow \gamma_a$	3	2
	$\gamma_a \leftrightarrow \gamma_3$	$\frac{3}{7}$	$\frac{7}{8}$
	$\gamma_3 \rightarrow \gamma_3$	$\frac{3}{7} \rightarrow 3$	$\frac{7}{8} \rightarrow 2$
$\gamma_a \leftrightarrow \gamma_3$	$\gamma_a \rightarrow \gamma_a$	$\frac{3}{7}$	$\frac{7}{8}$
	$\gamma_a \leftrightarrow \gamma_3$	$\frac{15}{11}$	$\frac{11}{10}$
	$\gamma_3 \rightarrow \gamma_3$	$\frac{3}{7} \rightarrow \frac{15}{11}$	$\frac{7}{8} \rightarrow \frac{11}{10}$
$\gamma_3 \rightarrow \gamma_3$	$\gamma_a \rightarrow \gamma_a$	$\frac{3}{7} \rightarrow 3$	$\frac{7}{8} \rightarrow 2$
	$\gamma_a \leftrightarrow \gamma_3$	$\frac{3}{7} \rightarrow \frac{15}{11}$	$\frac{7}{8} \rightarrow \frac{11}{10}$
	$\gamma_3 \rightarrow \gamma_3$	Arbitrary	Arbitrary

$g_{\parallel}$ value for the C_{4v} F^- center in CaF_2:Pr^{3+} (Ref. 9) of 2.72 MHz/G, a magnetic field of 10 kG would be sufficient to achieve exact coincidence of the $Z_1 \rightarrow {}^3P_0$ C_{4v} F^- center transition with the 476.5 nm argon laser line.

All the optical absorption transitions are confirmed by the excitation spectrum obtained when the laser pump frequency is continuously scanned while the fluorescence is monitored. Either a spectrometer is tuned to a particular transition, specifically to record the excitation spectrum of the corresponding single center, or broad band wavelength selection is used to detect all fluorescing centers present. For such centers laser excitation has vastly superior sensitivity compared to absorption, but

TABLE III. 14 K absorption transition wavelengths (in nm) from the Z_1 ground level to crystal-field levels of the ${}^3P_1$, ${}^3P_0$, and ${}^1D_2$ multiplets, for various C_{4v} centers in CaF_2:Pr^{3+} and SrF_2:Pr^{3+} crystals. Uncertainties are ±0.02 nm, unless otherwise incidated.

			Wavelength of absorption transition			
Crystal	Upper multiplet		F^-	H^-	D^-	T^-
CaF_2	${}^3P_1$		463.49	465.05	464.96	
			466.05	469.40	469.32	
	${}^3P_0$		477.14	480.28	480.36	
	${}^1D_2$	D_4	571.98	574.22	574.13	
		D_2	593.56	595.38	595.28	595.24
		D_1	594.10	596.68	596.69	596.69
SrF_2	${}^3P_1$		463.36	464.30	464.23	
			464.92	467.32	467.45	
	${}^3P_0$		476.52	478.94	479.00	
	${}^1D_2$	D_4	572.6±0.1	574.2±0.1	574.3±0.1	
		D_2	592.53			
		D_1	593.18	594.55	594.55	594.54

the observed line intensities depend on the fluorescence efficiencies of the various centers. Figure 3 shows the $^1D_2$ excitation spectrum for the C_{4v} F^- center in SrF_2:Pr^{3+}. The D_2 and D_4 crystal-field levels identified in absorption are indicated. The $Z_1 \rightarrow D_1$ excitation line is not apparent as this was the transition being monitored by the spectrometer. The broad phonon bands that were weakly visible in the absorption spectrum are now seen to comprise a number of distinct lines whose frequencies and energy shifts from the D_1 and D_2 crystal-field levels are listed in Table IV. These lines are transitions to vibonic states originating from lattice phonons coupling to the D_1 and D_2 levels. A large number of phonon features occur, with the energy of each given by the interval from the parent electronic line. A phonon with the same energy can couple to both D_1 and D_2 levels to give two vibronic transitions separated by the D_1-D_2 splitting. This is reflected in the equality of entries such as f and g in the second and third columns of Table IV.

Figure 3 was recorded with the spectrometer tuned to match exactly the $D_1 \rightarrow Z_1$ transition for the C_{4v} F^- center. By studying the intensity variation of the lines as the spectrometer is detuned slightly, it is deduced that the phonon band is relatively more efficient at pumping the background emission than is the D_4 crystal-field level. Accordingly the lattice phonons giving rise to the phonon structure are also responsible for the broad background features that are apparent in the fluorescence spectra. It is expected that the D_3 level would follow the same relative intensity variations as D_4, since they both resonantly excite the Pr^{3+} ion. As no other line in the phonon structure shows similar trends to D_4, the D_3 level does not appear to be one of the tabulated phonon vibronic features and its energy remains undetermined.

Fluorescence spectra from both the $^1D_2$ and $^3P_0$ multiplets to the various crystal-field levels of the $^3H_4$, $^3H_5$, $^3H_6$, $^3F_2$, $^3F_3$, $^3F_4$, and $^1G_4$ multiplets were recorded at 14 K, with selective excitation to the lowest crystal-field level, D_1, of the $^1D_2$ multiplet at 16858.3 cm^{-1}. In most cases 0.05 mol % Pr^{3+} crystals were studied and no evidence of cross relaxation to other distinct centers was observed at this Pr^{3+} concentration.

Representative spectra of the emission to the various multiplets are given in Fig. 4 with the lines labeled by the appropriate multiplet label for transitions from the D_1 level. When D_2 is the emitting level, this is labeled explicitly. Table V lists the energy levels derived from fluorescence for all the C_{4v} centers studied. Also included in this table is the polarization of each of the transitions observed from the D_1 and D_2 levels to levels of lower multiplets. The line evident at 16 876.7 cm^{-1} (Fig. 4) corresponds to the transition $D_2 \rightarrow Z_1$ which is at higher energy than the laser ($Z_1 \rightarrow D_1$ absorption). Its appearance indicates that a thermal population distribution is established between the D_1 and D_2 levels, under $Z_1 \rightarrow D_1$ excitation. The σ polarization of this line is not sufficient to establish the symmetry of the D_2 level itself.

The dominant emission line of the $^3P_0 \rightarrow {}^3H_4$ spectrum is the π-polarized $^3P_0 \rightarrow Z_5$ transition at 20 526 cm^{-1} (Fig. 4). As the single level of the $^3P_0$ multiplet must transform as the γ_1 irrep of C_{4v}, the terminating Z_5 level of this π-polarized transition transforms as the same irrep γ_1. A transition to this same Z_5 level is not observed from the D_1 level at 16 398 cm^{-1}, but a line at 16 416 cm^{-1} originating from the D_2 level some 18 cm^{-1} higher in energy is seen. This assignment of the 16 416 cm^{-1} line to the D_2 level is confirmed by the increase in its intensity with increasing temperature. It is concluded that the D_2 level has γ_1 symmetry. The same conclusions are

TABLE IV. Lattice vibronic features of C_{4v} F^- and hydrogenic centers in SrF_2:Pr^{3+} obtained from 14 K excitation spectra (monitoring D_1 to Z_1). Wave numbers as measured in air.

C_{4v} F^- center			C_{4v} hydrogenic centers				
	Vibronic intervals from				Vibronic intervals from		
Vibronic label in Fig. 2(a)	D_1 at 16858 cm^{-1}	D_2 at 16877 cm^{-1}	Vibronic label in Fig. 2(c)	D_1 at 16820 cm^{-1} in the C_{4v} D^- center	X_1 at 4222 cm^{-1} in the $C_{4v}H^-$ center	X_1 at 4218 cm^{-1} in the $C_{4v}D^-$ center	X_1 at 4215 cm^{-1} in the C_{4v} T^- center
a	147	129	*a*	165	170	173	174
b	181	163	*b*	177	180	181	182
c	190	172	*c*	187	187	189	190
d	204	186	*d*	244	218	223	224
e	233	215	*e*	291	287	291	292
f	281	263	*f*	303	298	303	303
g	300	282	*g*	318	313	313	
h	310	292					
i	322	304					
j	339	321					
k	405	387					
l	422	404					

reached from consideration of various other transitions to γ_1 or γ_5 symmetry levels and, in all cases, transitions from the D_2 level and from the single level of the $^3P_0$ multiplet show the same polarization. With the D_2 level identified as having γ_1 symmetry, the D_1 level is assigned to the $(^1D_2,\Gamma_3^+,\gamma_3)$ state and the D_2 level to $(^1D_2,\Gamma_3^+,\gamma_1)$. The energy level symmetry assignments given in Table V are then deduced directly from the σ or π polarization of the observed decay transitions, which give clearly distinct $x(yy)z:x(yx)z$ polarization ratios of 2:1 or 0:1, respectively (Table I). Additional transitions (identified by primed polarization labels in Table V) are all π-polarized magnetic-dipole transitions involving levels of γ_2 symmetry and these have observed $x(yy)z:x(yx)z$ polarization ratios of 1:0 (Table I). The spectra also include some vibronic features associated with lattice phonons. Of the many transitions observed, two to the Y_2 (Γ_3^+,γ_1) level of the $^3H_5$ multiplet are noteworthy for showing a large intensity difference, the π-polarized transition from D_2 being particularly strong, while the corresponding transition from $^3P_0$ is just visible.

A strong sharp line at 14 353 cm^{-1} appearing in the emission spectrum from $^1D_2$ for some crystals is attribut-

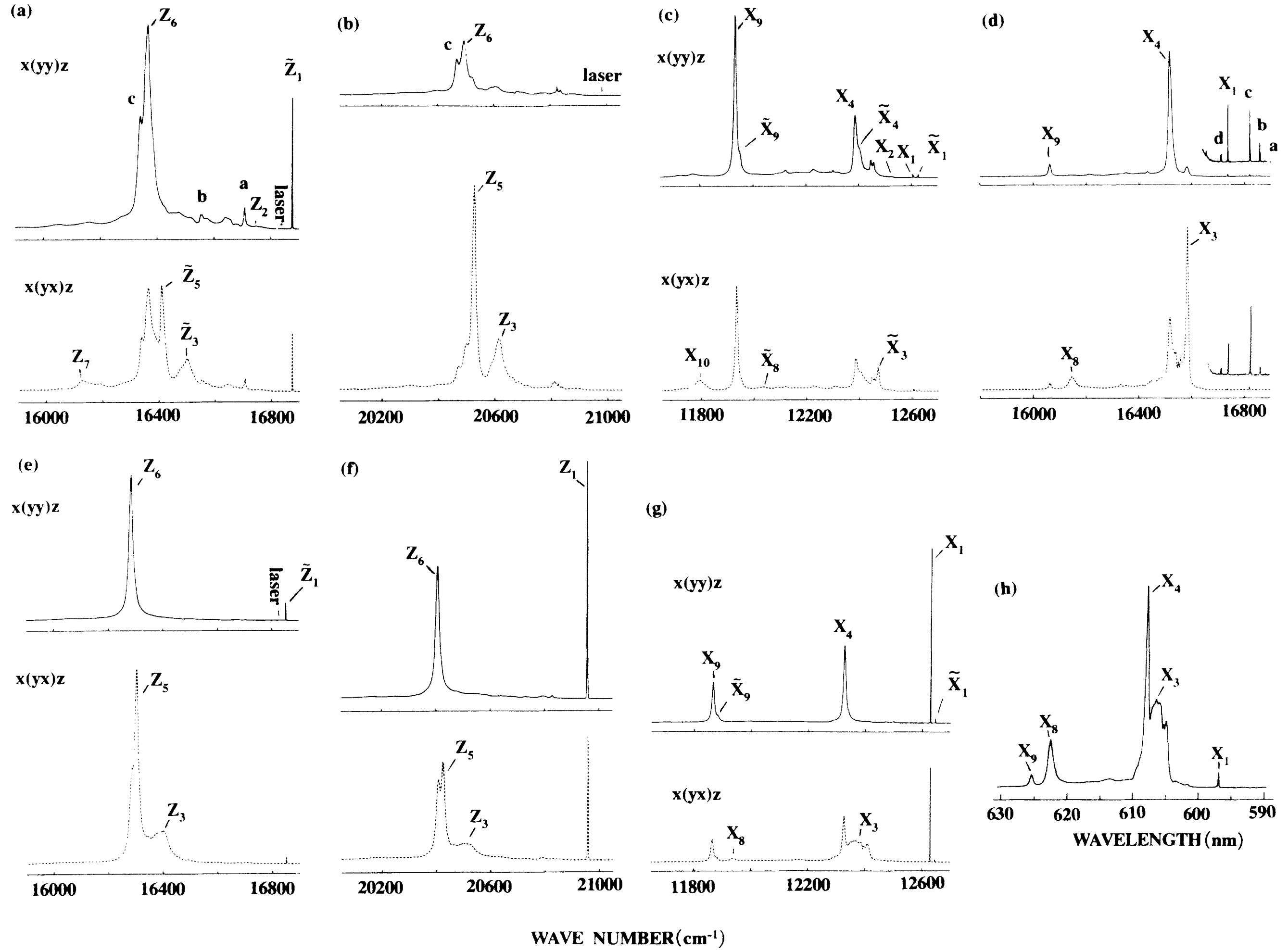

FIG. 4. 14 K polarized $[x(yy)z$ and $x(yx)z]$ fluorescence to the $^3H_4(Z)$ and $^3H_6(X)$ multiplets from the $^1D_2$ multiplet [(a), (c), (e), and (g)] and from the $^3P_0$ multiplet, either directly pumped [(b) and (d)] or by upconversion [(f) and (h)]. The spectra were obtained by selective excitation of the C_{4v} F^- center in ⟨100⟩ oriented crystals of the following: (a) and (c), SrF$_2$:Pr^{3+} (laser at 16858.2 cm^{-1} in air); [(b) and (d)], SrF$_2$:Pr^{3+} (laser at 20985.4 cm^{-1} in air); and, [(e)–(h)], CaF$_2$:Pr^{3+} (laser at 16832.1 cm^{-1} in air). Transitions are identified by their terminating level and those originating from the D_2 level of the $^1D_2$ multiplet are so identified. Lines labeled "a", "b" or "c" in (a) and (b) are lattice phonon vibronic features, while those labeled "a" to "d" in (d) arise from $^1D_2 \rightarrow {}^3H_4$ transitions for C_{4v} F^- and other centers.

TABLE V. Energy levels (±1 cm^{-1} in air) for C_{4v} F^- and D^- centers in SrF_2 and CaF_2 at 10 K. Symmetry assignments are also given based on the observed electric dipole (σ or π) or magnetic dipole (π') polarizations of transitions from the D_1 (or $^3P_0$) level and, for the F^- centers, from the D_2 level.

Energy level label and symmetry assignment			C_{4v} F^- center						C_{4v} D^- center			
			SrF_2			CaF_2			SrF_2		CaF_2	
				From D_2 (or $^3P_0$)	From D_1		From D_1	From D_2		From D_1		From D_1
	U_7	γ_1	7286	(π)	–	–	–	–	–	–	7307	π
	U_6	γ_5	7260	σ	σ	7350	σ	–	7245	σ	7343	σ
	U_5	γ_3	7206	π	–	–	–		7208	π	–	–
	U_4	γ_2	7146	(π')	π'	–	–	–	–	–	–	–
$^3F_4$	U_3	γ_4	–	–	–	–	–	–	6963	π'	7017±5†	–
	U_2	γ_5	7024	σ	σ	7068	σ	–	6999	σ	7040	σ
	U_1	γ_1	6966	(π)	π	6980	π	–	6938	π	6947	π
	V_5	γ_3	6821	π	–	6900	–	π	6780	π	–	–
	V_4	γ_5	6762	σ	σ	6840	σ	σ	6740	σ	6820	σ
$^3F_3$	V_3	γ_2	6702	(π')	π'	6754	π'	–	6672	π'	6719	π'
	V_2	γ_4	6565	π'	–	6607	–	π'	6556	π'	–	–
	V_1	γ_5	6484	σ	σ	6500	σ	σ	6461	σ	6473	σ
	W_4	γ_3	5394	π	–	5478±2	–	π	5380	π	5448†	–
	W_3	γ_5	5308	σ	σ	5387	σ	σ	5290	σ	5357	σ
$^3F_2$	W_2	γ_1	5275	π	π	5332	π	–	5246	π	5293	π
	W_1	γ_4	5225	π'	–	–	–	–	–	–	–	–
	X_{10}	γ_3	5064±2	π	–	–	–	–	5057	π	–	–
	X_9	γ_5	4923	(σ)	σ	4954	σ	σ	4923	σ	4967	σ
	X_8	γ_1	4840	(π)	π	4896	π	–	4831	π	4869	π
	X_7	γ_4	–	–	–	–	–	–	–	–	–	–
	X_6	γ_3	–	–	–	–	–	–	–	–	–	–
$^3H_6$	X_5	γ_1	4555	(π')	–	–	–	–	–	–	–	–
	X_4	γ_5	4471	σ	σ	4508	σ	–	4480	σ	4528	σ
	X_3	γ_1	4405	(π)	π	4468±10	π	–	4441	π	4476	π
	X_2	γ_4	4330	π'	–	–	–	–	–	–	–	–
	X_1	γ_5	4250	σ	σ	4205	σ	σ	4218	σ	4163	σ
	Y_8	γ_4	–	–	–	–	–	–	–	–	–	–
	Y_7	γ_5	2668±2	σ	–	2738	–	–	2667±3	–	2723	σ
	Y_6	γ_2	2359	π	–	–	–	–	–	–	–	–
	Y_5	γ_5	2334	σ	σ	2399	σ	σ	2339	σ	2425±20	σ
	Y_4	γ_3	2292	π	–	2324	–	π	2305	π	–	–
$^3H_5$	Y_3	γ_5	2285	σ	–	2270	σ	σ	2236	σ	2206	σ
	Y_2	γ_1	2221	π	π	2211	π	–	2199	π	2183	π
	Y_1	γ_2	2195	(π')	π'	2189	π'	–	2175	π'	2164	π'
	Z_7	γ_3	726±2	π	–	728	–	π	736±2	π	834±5†	–
	Z_6	γ_5	490	σ	–	552	σ	–	499	σ	559	σ
	Z_5	γ_1	461	(π)	π	534	π	–	467	π	559±20	–
$^3H_4$	Z_4	γ_2	–	–	–	484	π'	–	–	–	–	–
	Z_3	γ_1	373±2	(π)	π	447±10	π	–	387±2	π	463	π
	Z_2	γ_4	108	π'	–	–	–	–	139±3†	–	195±5†	–
	Z_1	γ_5	0	σ	σ	0	σ	σ	0	σ	0	σ

† Position inferred from energy of associated X,Y local mode vibronic.

ed to the $(^5D_0)^1\Gamma_{1g} \rightarrow (^7F_1)^3\Gamma_{4g}$ transition of the Sm^{2+} ion.[11] Excitation of the Sm^{2+} emission is unavoidable as Sm^{2+} ions have a broad absorption profile extending from 15 000 to 20 000 cm^{-1}, in the same spectral region as the sharp $^1D_2$ absorption transitions of Pr^{3+}. The origin of the Sm^{2+} impurity can be traced to the praseodymium dopant material used in the crystal growth. The occurrence of Sm^{2+} emission is more apparent in the spectra of C_{4v} hydrogenic centers (Sec. IV) as these have much weaker fluorescence.

Fluorescence transitions to levels of the $^1G_4$ multiplet were observed for SrF_2 by exciting the $^3P_0$ level with the 476.5-nm argon laser line (Fig. 2). In addition to the identified Pr^{3+} ion transitions, the $R_1 \rightarrow Z$ lines of the C_{4v} center of Nd^{3+} were also apparent in the 11 600 cm^{-1} region.[12] As for the case of Sm^{2+}, Nd^{3+} ions are present as trace impurities in the praseodymium dopant material used in the crystal growth.

C. The C_{4v} F^- center in CaF_2

In common with most other rare-earth ions in fluorite crystals, the optical absorption spectrum of Pr^{3+} in the CaF_2 host contains more structure than in the SrF_2 host. Figure 1 shows the absorption to the $^3P_0$, $^3P_1$, and $^1D_2$ multiplets for a 0.02 mol % Pr^{3+}-doped crystal. Only the C_{4v} F^- center was singled out for laser excitation study. Figure 3 shows the $^1D_2$ excitation spectrum for the C_{4v} F^- center in CaF_2, with the D_1, D_2, and D_4 crystal-field levels indicated. Although less-well resolved than was the case for the C_{4v} F^- center in SrF_2:Pr^{3+} a broad band of phonon structure is present in the region between the D_2 and D_4 transitions. Spectra of the emission from both the $^1D_2$ and $^3P_0$ multiplets to various crystal-field levels of the $^3H_4$, $^3H_5$, $^3H_6$, $^3F_2$, $^3F_3$, and $^3F_4$ multiplets were recorded for the C_{4v} F^- center. Selective excitation of the $^1D_2$ multiplet was to the lowest crystal-field level at 16 832.2 cm^{-1}. The $^3P_0$ emission was excited using the tunable pulsed dye laser with resultant weaker fluorescence. An alternative was excitation with the 457.9 nm argon laser line as the subsequent emission is mostly from the C_{4v} F^- center. Other argon lines can then be used to identify features not associated with the C_{4v} F^- center. It was also possible to obtain weak $^3P_0$ emission spectra through upconversion processes when pumping the $^1D_2$ multiplet (Sec. VI).

Zeeman studies[9] have identified the D_1 level in CaF_2:Pr^{3+} as having γ_1 symmetry, in contrast to the γ_3 assignment (Sec. III B) for the C_{4v} F^- center in SrF_2. As the fluorescence transitions leading to the D_1, D_2 assignments for SrF_2 are not observed with the same polarization in the CaF_2 spectra, the assignment of a different symmetry to the D_1 level is confirmed.

Representative spectra of the polarized emission to various multiplets are given in Fig. 4, while Table V summarizes the energy-level assignments made, together with the transition polarizations from D_1 used for the assignments. In all cases, the polarization ratios are in complete agreement with the level symmetries given. Since both the D_1 and $^3P_0$ levels transform as the same symmetry irrep, vis. γ_1, the emission spectra do not show the diversity of transitions and levels observed for the C_{4v} F^- center in SrF_2:Pr^{3+} and the energy-level tabulation derived is somewhat less complete.

As for SrF_2:Pr^{3+}, the transitions to the $^3H_5$ multiplet are partially overlapped by transitions of the Sm^{2+} ion. In CaF_2, the principal line of Sm^{2+} observed[11] is the transition $(4f^55d)A_{1u} \rightarrow (4f^6)^7F_0$ at 14 114 cm^{-1}.

The transitions to the $^3H_6$ multiplet also show a broad band ascribed to lattice phonons coupled to the X_1 level. A band of this type appears in this multiplet for all the C_{4v} centers studied.

The relative intensities of corresponding magnetic-dipole transitions to levels of the $^3F_3$ multiplet in CaF_2 and SrF_2 are very different because of the reversed symmetries of the D_1 and D_2 levels in the two host crystals. The magnetic-dipole-allowed transition $D_1(\gamma_3) \rightarrow V_2(\gamma_4)$ in SrF_2:Pr^{3+} is readily apparent while the corresponding transition $D_2(\gamma_3) \rightarrow V_2(\gamma_4)$ in CaF_2Pr^{3+} is much weaker because it requires thermal population of the D_2 level for its intensity. For the same reason, the $D_1(\gamma_1) \rightarrow V_3(\gamma_2)$ transition in CaF_2:Pr^{3+} is much stronger than the $D_2(\gamma_1) \rightarrow V_3(\gamma_2)$ transition in SrF_2:Pr^{3+}.

IV. SPECTROSCOPY OF Pr^{3+} IN THE ALKALINE EARTH FLUORIDES AFTER HYDROGENATION

It is well known that H^- ions, and the corresponding isotopes D^- and T^-, can be introduced into fluorite type crystals and participate in charge compensation of any trivalent rare-earth ions present.[13] The simplest and most well-characterized hydrogenic center is the C_{4v} H^- charge-compensated center produced by the substitution of an H^- ion for the interstitial charge compensating F^- ion of the analogous C_{4v} F^- center.

In hydrogenic centers, the optical spectra are more complex as the electron-phonon interaction between the rare-earth electronic states, and the hydrogenic ion localized modes gives rise to several additional spectral features,[14] which include the following: (a) the occurrence of local-mode phonon vibronic lines separated from the (zero-phonon) electronic transitions of the rare-earth ion by energy intervals corresponding to the energies of the local-mode phonons. (b) The existence of isotope shifts (of approximately 1 cm^{-1}) in the electronic levels of the rare-earth ion for the H^-, D^-, and T^- charge compensated centers. (c) The occurrence of vibronic shifts (of approximately 1 cm^{-1}) in the local-mode energies as measured for different electronic transitions of the rare-earth ion.

The C_{4v} H^- center local-mode phonon energies, appropriate to the rare-earth ion ground electronic level, have been measured by infrared absorption[10] and are used in the analysis of the relatively complicated local-mode vibronic structure found in the Pr^{3+} fluorescence spectra detailed in Secs. IV A 2 and IV B 2.

The selection rules for polarized emission to the local-mode phonon vibronic levels can be derived in a similar manner to that used for the electronic transitions (Sec. III A), using both the electronic level and local-mode phonon symmetry labels. As the longitudinal (Z) and transverse (X,Y) local-mode phonons transform as the γ_1 and γ_5 irreps of C_{4v}, respectively, the polarization behavior of the Z local-mode vibronic transitions is necessarily the same as that of the parent electronic transition, while the (X,Y) local-mode vibronic transitions have a different polarization behavior. The (X,Y) vibronic states associated with any of the $\gamma_{a'}$ ($a'=1$, 2, 3, or 4) electronic states have γ_5 symmetry and consequently transitions from (or to) a $\gamma_{a'}$ state are σ polarized. The (X,Y) vibronic levels associated with a γ_5 electronic state comprise a set of four vibronic states ($\gamma_5 \times \gamma_5 = \gamma_1 + \gamma_2 + \gamma_3 + \gamma_4$), and a π-polarized transition will be observed from a $\gamma_{a'}$ state to the level of this set with the same symmetry (Table I). Often the observation of (X,Y) vibronic transitions can be used to infer the energies of rare-earth electronic transitions in those cases where these are electric-dipole forbidden and hence absent from the spectra.

The C_{4v} H^- center of Pr^{3+} in both CaF_2 and SrF_2 was first observed through identification of local-mode infrared lines,[13] while preliminary optical studies of these crystals recorded transitions to the $^3P_0$ and $^3P_1$ levels for both H^- and D^- varieties of the C_{4v} center.[10]

The fluorescence spectra measured in this work have been used to identify crystal-field levels of the $^3H_4$, $^3H_5$, $^3H_6$, $^3F_2$, $^3F_3$, and $^3F_4$ multiplets for the H^-, D^-, and T^- varieties of the C_{4v} centers in both CaF_2 and SrF_2. In addition, transitions have been observed to many local-mode levels in these multiplets which yield the local-mode energies of the H^-, D^-, and T^- ions.

The spectroscopy of the C_{4v} hydrogenic centers is now described separately for SrF_2 and CaF_2.

A. The C_{4v} hydrogenic center in SrF_2:Pr^{3+}

1. *Absorption and excitation spectra*

Absorption transitions to the $^1D_2$, $^3P_0$, and $^3P_1$ multiplets were recorded for both SrF_2:Pr^{3+}:H^- (Fig. 1) and SrF_2:Pr^{3+}:D^- crystals. A large number of new absorption lines are observed compared to the parent crystals. The assignment of these new lines is based on the observation of isotope shifts between the spectral lines in the H^- and D^- crystals and by the observation (revealed by related fluorescence spectra measurements) of local-mode vibronic lines at the expected energy intervals. Transitions to the $^3P_0$, $^3P_1$, and $^1D_2$ multiplet levels of the Pr^{3+} ion in the C_{4v} H^- center are indicated in Fig. 1, and this center is the major hydrogenic center observed. Lines of a number of other hydrogenic centers are also present. Some of these belong to centers containing multiple hydrogenic ions and the spectroscopy of these centers [$C_s(1)$ to $C_s(4)$] has already been published.[5] Table III summarizes the absorption transitions observed for all the C_{4v} hydrogenic centers measured, the C_{4v} T^- center data having been obtained from excitation spectra. Absorption spectra recorded at 85 K show no evidence of transitions originating from the first excited level (Z_2) for any of the C_{4v} centers, placing a lower limit of 100 cm^{-1} for the energy of the Z_2 level above the ground level (Z_1).

Also absent from the $^1D_2$ absorption spectrum is the transition to the second crystal-field level, D_2, of this multiplet. This level also was not apparent in any of the fluorescence spectra (Sec. IV A 2). For the corresponding C_{4v} hydrogenic centers in CaF_2, the D_2 level appeared, albeit weakly, 40 cm^{-1} above D_1 (Sec. IV B 1).

The excitation spectra reveal many additional absorption features (Fig. 3). The D_1 and D_4 electronic levels appear with polarization appropriate to their symmetry assignments, and a phonon band is present, with features whose energy separations from the D_1 level are tabulated in Table IV.

When recorded at high sensitivity the excitation spectrum of the C_{4v} D^- center in SrF_2:Pr^{3+} (Fig. 3) reveals a number of extra lines superposed on the high-energy wing of the Z_1 to D_4 transition. As for the emission spectra, local-mode vibronic lines occur in absorption, or excitation in this case, at energy intervals matching the D^- local-mode vibrational frequencies. The local-mode vibrational intervals from the Z_1 to D_1 transition identify two excitation lines as the (X,Y) and Z local-mode vibronic lines associated with the D_1 electronic level. At higher energies additional weaker structure that can be assigned as D^- local modes coupling to the D_4 crystal-field level and as second harmonic D^- local modes coupling to the D_1 level is evident. In particular the transitions to vibronic levels of all three second harmonic combinations XX, XZ, and ZZ are identified (Table VI).

2. *Fluorescence spectra of the hydrogenic centers in SrF_2*

Fluorescence spectra comprising transitions to crystal-field levels of the $^3H_4$, $^3H_5$, $^3H_6$, $^3F_2$, $^3F_3$, and $^3F_4$ multiplets were recorded for selective excitation of the $^1D_2$ multiplet and, in some cases, the $^3P_0$ multiplet. The spectral range scanned for each multiplet was extended to include coverage of all possible local-mode vibronic lines whose energies are many hundred cm^{-1} lower than their parent electronic lines (Fig. 5 and Table VII). The electronic lines are labeled by the terminating level of the transition, while the local-mode lines are also labeled by X (indicating X,Y) or Z, as appropriate. The electronic and local-mode vibronic level energies are summarized in Tables V and VII respectively, together with their transition polarization (σ or π) from the D_1 level. A direct transition to the Z_2 crystal-field level has not been observed for any of the C_{4v} hydrogenic centers; however, an energy can be inferred for this level from the observation of its (X,Y) local-mode vibronic lines, as indicated in Table VII.

For the interpretation of the polarization of the ob-

TABLE VI. D^- local mode energies (± 2 cm^{-1} in air, unless otherwise stated) deduced from 14 K excitation spectra of the D^- C_{4v} center, $^1D_2$ multiplet. Local mode assignments are given as X for (X,Y) type vibrational modes, Z for the Z modes, or as XX, XZ, or ZZ for the various possible second harmonic local modes.

Crystal	Parent electronic level	Electronic level energy (± 0.5 cm^{-1} in air)	D^- vibronic level mode and energy	
CaF_2	D_1	16759.1	X:	722±1
			Z:	810±1
			ZZ:	1620
	D_2	16798.8	X:	721±1
	D_4	17417.6	X:	721
			Z:	804
SrF_2	D_1	16819.4	X:	664.0±0.5
			Z:	686.4±0.5
			XX:	1332
			XZ:	1342
			ZZ:	1364
	D_4	17412.5	X:	604
			Z:	676

served fluorescence transitions, an assignment of the symmetries of the D_1 and D_2 levels of the $^1D_2$ multiplet is required. The observation that transitions from the $^3P_0$ level had the same polarization as those from D_2 sufficed to establish the D_2 level as having γ_1 symmetry in the case of the C_{4v} F^- center. No fluorescence or absorption transitions involving the D_2 level have been observed for any of the C_{4v} hydrogenic centers in SrF_2 and its position is unknown. Predicting its energy by comparison with the other C_{4v} centers is not straightforward because of the reversal of symmetry assignments of the D_1 and D_2 levels between the C_{4v} F^- centers in SrF_2 and CaF_2. In SrF_2 the splitting of the two crystal-field levels of the $^3P_1$ multiplet increases from 72.4 cm^{-1} for the C_{4v} F^- center to 148.3 cm^{-1} for the C_{4v} D^- center indicating that the second-degree axial crystal-field term increases by a factor of 2 for D^- replacing F^-. The separation of the D_1 and D_2 levels is the net effect of both second-degree and fourth-degree C_{4v} crystal field terms,[15] and these are not known sufficiently precisely to enable accurate predictions of the D_1 to D_2 splitting for the D^- center. There is a strong possibility that the D_1 and D_2 levels are almost coincident in energy as modified hydrogenic centers in mixed 1% Ca^{2+} in SrF_2:0.05% Pr^{3+} crystals show closely spaced D_1 and D_2 lines.[16] Having the D_1 and D_2 levels almost coincident would also resolve the conflict apparent in the assignment of the symmetry of the D_1 level. π-polarized magnetic dipole transitions observed from both the $^3P_0$ and D_1 levels to the $Y_1(^3H_5,\Gamma_4^+,\gamma_2)$ level indicate that D_1 transforms as γ_1; however, the observation of several π-polarized transitions terminating on γ_3 levels (Table V) suggests a γ_3 symmetry for D_1.

The spectra of the hydrogenic centers in the $^3H_5$ multiplet region show quite prominently the Sm^{2+} line[11] at 14 353 cm^{-1}. The increase in its relative strength is partially because of the lower fluorescence efficiency of hydrogenic centers compared to their F^- counterparts and partially because the Sm^{2+} ion concentration is increased through reduction of Sm^{3+} to Sm^{2+} in the hydrogenation process.

The lowest level Y_1 of the $^3H_5$ multiplet is determined to have γ_2 symmetry by the polarization observed for the $D_1 \rightarrow Y_1$ transition, appropriate for a magnetic dipole transition. This assignment is the same as for the corresponding transition of the analogous C_{4v} F^- center.

The fourfold degenerate set of (X,Y) vibronic levels associated with the Z_1 ground electronic state shows a splitting into two components (Fig. 5). This splitting is attributed to the coupling of the (X,Y) local-mode phonon to the Pr^{3+} electronic states by the electron-local-mode phonon interaction.[17] The splitting of (X,Y) vibronic levels associated with γ_5 electronic states is enhanced in the case of the Z_1 ground state by the close proximity in energy of the $Z_7(\gamma_3)$ electronic level. The biggest splitting is observed for the C_{4v} D^- center where the (X,Y) vibronic set is centered at 663 cm^{-1}, only 73 cm^{-1} below that of the $Z_7(\gamma_3)$ electronic level (Table VII). The observation of transitions from levels of $\gamma_{a'}$ symmetry to more than one (X,Y) vibronic component, however, indicates some departure from strict C_{4v} symmetry. Calculations of these (X,Y) splittings, similar to those detailed for Ce^{3+} C_{4v} H^- centers in CaF_2 and SrF_2,[17] will be reported elsewhere.

Transitions associated with second harmonic local-mode vibrations of the hydrogenic ions have been observed for all the C_{4v} hydrogenic centers. In C_{4v} symmetry sites, the hydrogenic ions have five-second harmonic levels as the anharmonic oscillator potential[13] splits the

TABLE VII. Hydrogenic local mode energies at 10 K deduced from transitions between the D_1 electronic level of the $^1D_2$ multiplet and vibronic levels of the $^3H_4$ multiplet for hydrogenic C_{4v} centers. The observed polarization of the transition from D_1 to each vibronic level is also indicated. All energies are in air wave numbers (± 1 cm^{-1} unless otherwise indicated).

Crystal	Electronic state symmetry and polarization	$C_{4v}H^-$		$C_{4v}D^-$		$C_{4v}T^-$	
		Electronic level energy	Vibronic level, mode energy and polarization	Electronic level energy	Vibronic level, mode energy and polarization	Electronic level energy	Vibronic level, mode energy and polarization
SrF_2	$Z_1(\gamma_5)$, σ	0	x: 921.6 ± .5 (π) 925.1 ± .5 (π) z: 939.6 ± .5 (σ) xx: 1846.2 ± .5 (σ) 1849.2 ± .5 (σ) 1851.2 ± .5 (σ) xz: 1857.7 ± .5 (π) zz: 1870.7 ± .5 (σ)	0	x: 658.4 ± .5 (π) 666.9 ± .5 (π) z: 684.9 ± .5 (σ) xx: 1322.9 ± .5 (σ) xz: 1342.4 ± .5 (π) zz: 1363.9 ± .5 (σ)	0	x: 558 (π) z: 575 (σ) xx: - xz: 1131 (π) zz: 1144 (σ)
	$Z_2(\gamma_4)$, *	138±5	x: 914 ± 5 (σ) z: 932 ± 5 (σ) xx: 1846 ± 5 (σ)	139 ± 3	x: 662 ± 3 (σ) xz: 1340 ± 3 (π)	137 ± 3	x: 558 ± 3 (σ)
	$Z_3(\gamma_1)$, π	386±2	x: 916 ± 5 (σ) z: 934 ± 5 (π)	387 ± 2	x: 660 ± 5 (σ) z: 682 ± 5 (π) xz: 1342 ± 5 (σ)	387 ± 2	x: 550 ± 5 (σ) z: 570 ± 5 (π)
	$Z_5(\gamma_1)$, π	466	x: 919 (σ) z: 939 (π)	467	x: 663 (σ) z: 683 (π) xz: 1345 ± 2 (σ) zz: 1359 ± 2 (π)	467	x: 553 ± 2 (σ) z: 575 ± 2 (π)
	$Z_6(\gamma_5)$, σ	498	z: 939 (σ)	499	z: 683 (σ) zz: 1359 (σ)	498	z: 574 (σ) zz: 1142 ± 5 (σ)
	$Z_7(\gamma_3)$, π	729±2	x: 915 ± 3 (σ)	736±2	x: 663 ± 2 (σ)	732 ± 2	x: 554 ± 2 (σ)
CaF_2	$Z_1(\gamma_5)$, σ	0	x: 996.5 ± .5 (π) 997.3 ± .5 (π) 1002.5 ± .5 (π) z: 1117.5 ± .5 (σ) xx: 1992.3 ± .5 1998.3 ± .5	0	x: 722.8 ±.5 (π) z: 808.1 ±.5 (σ) xx: 1435 (σ) 1444 (σ) xz: 1528 (π) zz: 1606 (σ)	0	x: 606 (π) z: 673 (σ) xx: - xz: 1275 (π) zz: 1338 (σ)
	$Z_2(\gamma_4)$, *	191±5	x: 998 ± 5 (σ)	195 ± 5	x: 707 ± 10 (σ) xx: 1442 ± 10 (π) xz: 1522 ± 5 (σ)	192 ± 5	x: 601 ± 5 (σ) xz: 1275 ± 5 (σ)
	$Z_3(\gamma_1)$, π	462	x: 994 ± 5 (σ) z: 1113 ± 5 (π)	463	x: 713 ± 5 (σ) z: 805 ± 5 (π) xx: - xz: 1527 ± 5 (σ) zz 1610 ± 5 (σ)	464	x: - z: 671 ± 10 (π) - xx: 1204 ± 10 (σ) xz: 1277 ± 10 (σ)
	$Z_6(\gamma_5)$, σ	560	x: 993 (π) z: 1116 (σ)	559	x: - z: 806 (σ)	559	x: - z: 670 ± 5 (σ) zz: 1335 ± 2 (σ)
	$Z_7(\gamma_3)$, *	821±5	x: 997 ± 5 (σ)	834 ± 5	x: 723 ± 5 (σ)	831 ± 5	x: 606 ± 5 (σ)

* Position inferred from position of local mode vibronic levels.

transverse (XX) vibration into three components. Three of these second harmonic transitions are infrared active and have been measured by infrared absorption[13] for the C_{4v} H^- centers in CaF_2 crystals containing Gd^{3+}, Tm^{3+}, and Y^{3+}. All five-second harmonic frequencies are present in the Pr^{3+}-H^- vibronic spectra measured here (again indicating departure from C_{4v} symmetry) and their energies are included in Table VII, together with the polarization of the particular vibronic transitions observed and the local-mode (X, Z, XX, XZ, or ZZ) assignment. The polarizations of the vibronic levels are generally consistent with electric-dipole selection rules and their parent electronic level symmetry assignment, although occasional discrepancies occur for weaker features.

If there is some departure from strict C_{4v} symmetry for these centers, one might expect this to show up as a split-

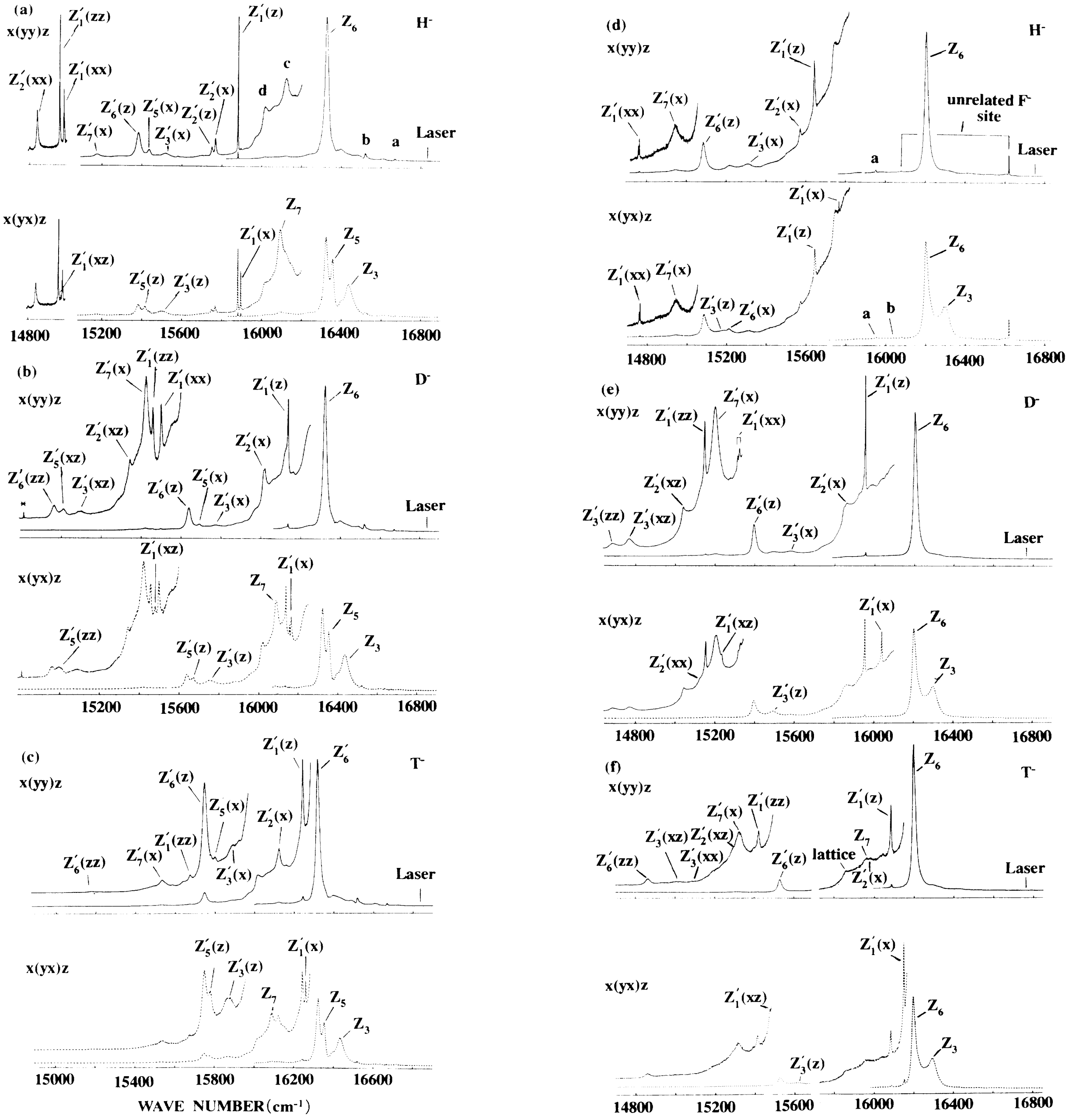

FIG. 5. Selective-excitation 14 K polarized fluorescence from the $^1D_2$ multiplet for C_{4v} hydrogenic centers in ⟨100⟩ oriented $SrF_2:Pr^{3+}$ crystals: (a) $SrF_2:Pr^{3+}:H^-$ (excitation at 16819.4 cm^{-1} in air), (b) $SrF_2:Pr^{3+}:D^-$ (excitation at 16819.4 cm^{-1} in air), (c) $SrF_2:Pr^{3+}:T^-$ (excitation at 16819.7 cm^{-1} in air); and in ⟨100⟩ oriented $CaF_2:Pr^{3+}$ crystals: (d) $CaF_2:Pr^{3+}:H^-$ (excitation at 16759.4 cm^{-1} in air), (e) $CaF_2:Pr^{3+}:D^-$ (excitation at 16759.1 cm^{-1} in air), (f) $CaF_2:Pr^{3+}:T^-$ (excitation at 16759.1 cm^{-1} in air). Assigned electronic transitions are identified by their terminating level, while assigned local-mode vibronic transitions include the local mode assignment. Lines labeled "a" to "d" are lattice phonon vibronic features.

ting of the $\gamma_5(C_{4v})$ ground state. Recent infrared absorption results do indeed indicate a ground-state splitting of about 0.3 cm^{-1} for the C_{4v} F^- centers in both CaF_2 and SrF_2 containing 0.01% of Pr^{3+}. The higher Pr^{3+} concentration (0.05%) and the bandwidth of the dye laser used here would appear to have precluded the direct observation of such a splitting in this work (see further comment in Sec. V).

A special case of a local-mode vibronic line having comparable intensity to its parent electronic transition is the transition to the lowest level, X_1, of the $^3H_6$ multiplet (Fig. 6). The intensities of both the $D_1 \rightarrow X_1$ and $^3P_0 \rightarrow X_1$ electronic transitions are unusually weak for electric-dipole transitions.

Several lines falling in the $^3P_0 \rightarrow {}^3H_6$ spectral region are actually $^1D_2 \rightarrow {}^3H_4$ transitions, identified by their en-

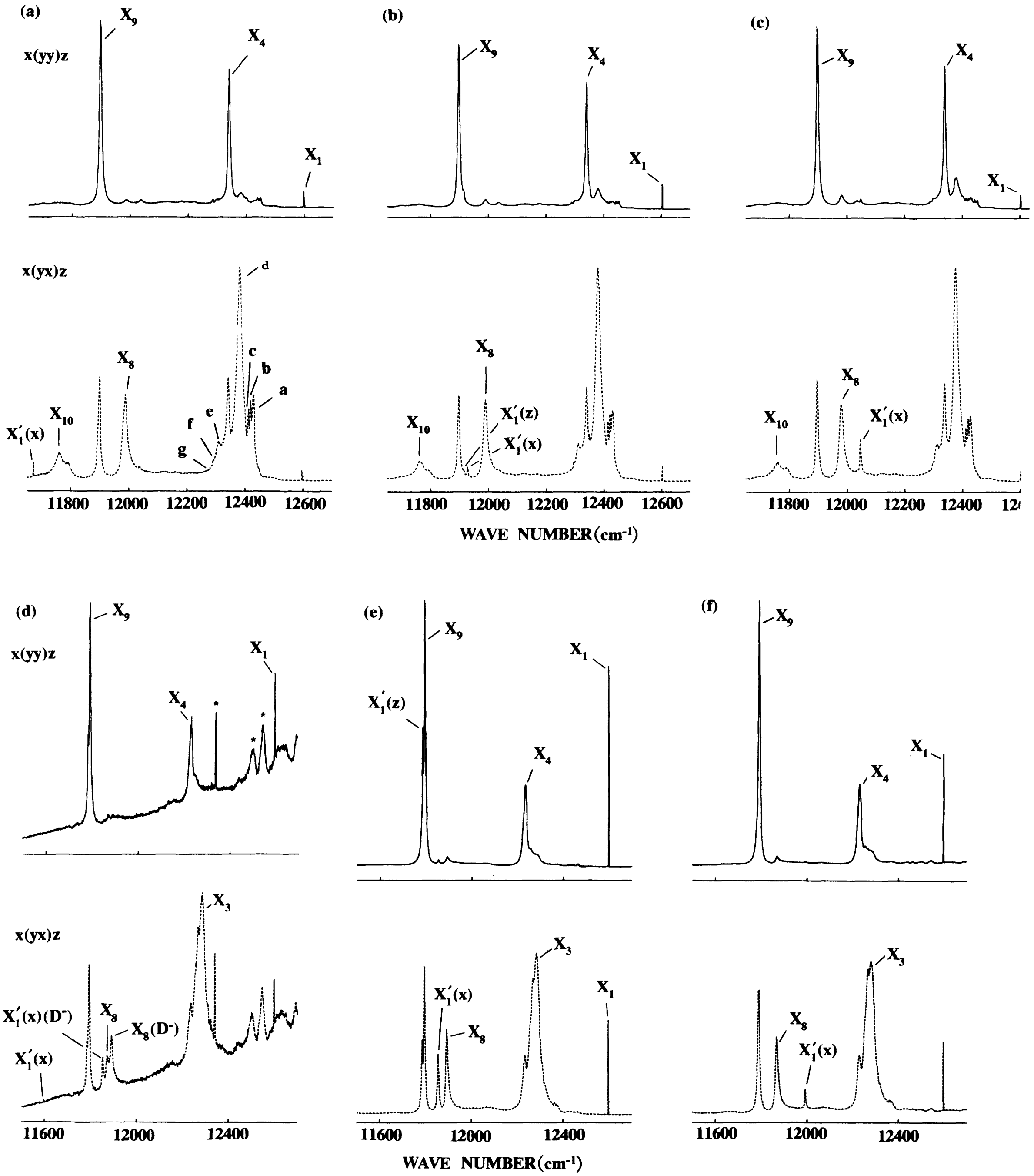

FIG. 6. Selective-excitation 14-K polarized fluorescence spectra from the $^1D_2$ multiplet to the $^3H_6(X)$ multiplet for the same C_{4v} centers and excitation energies as detailed in Fig. 5. Lines labeled "a" to "g" are lattice phonon vibronic features and lines labeled* do not originate from a C_{4v} center.

ergies and confirmed through their longer fluorescence lifetimes. Their presence indicates a mechanism, via the hydrogenic ions, for populating the $^1D_2$ multiplet after excitation of the $^3P_0$ multiplet as emission from $^1D_2$ following $^3P_0$ excitation is practically nonexistent for the C_{4v} F^- centers.

All the transitions to the $^3F_3$ multiplet are observed, with those to the V_2 and V_3 levels having a polarization consistent with magnetic-dipole transitions to both levels. However, the identification of both these transitions as magnetic dipole would require the D_1 emitting level to have both γ_1 and γ_3 symmetry (again supportive of near coincidence of the D_1 and D_2 levels).

The transitions to the V_1 and V_5 levels are exceptional in the case of the C_{4v} H^- center in showing structure of two components separated by 0.3 and 0.4 cm^{-1}, respectively.

B. The C_{4v} hydrogenic center in CaF$_2$:Pr^{3+}

1. *Absorption and excitation spectra*

The optical absorption spectrum for deuterated crystals of CaF$_2$:Pr^{3+} is presented in Fig. 1, transitions belonging to the C_{4v} center being so identified. Absorption transitions of several lower-symmetry, multiple-hydrogenic-ion centers are also present. Data for all C_{4v} hydrogenic centers in CaF$_2$ are included in Table III.

A weak transition is observed to the D_2 level of the $^1D_2$ multiplet at 16 798.8 cm^{1-}. This places the D_2 level 40 cm^{-1} above D_1, as compared to 15 cm^{-1} for the C_{4v} F^- center, indicating a doubling of the axial crystal-field. A similar increase is apparent for the splitting ($0.3B_0^2$) of the two levels of the $^3P_1$ multiplet from 118 cm^{-1} for the C_{4v} F^- center to 200 cm^{-1} for the D^- center. The replacement of the F^- charge-compensating ion by a hydrogenic ion thus increases the second-degree axial crystal-field parameter B_0^2 by about a factor of 2. The symmetries of the D_1 and D_2 crystal-field levels for the hydrogenic centers in CaF$_2$ are found to be the same as for the corresponding F^- center, with D_1 and D_2 having γ_1 and γ_3 symmetry, respectively.

The weak transition to the D_2 level is more clearly shown in the excitation spectrum (Fig. 3). In addition to the D_1, D_2, and D_4 crystal-field levels, a broad band ascribed to lattice phonons is present, as well as a number of lines attributed to other Pr^{3+} centers.

As for the C_{4v} D^- center in SrF$_2$:Pr^{3+}, excitation transitions to local-mode vibronic levels associated with the D_1 and D_2 crystal-field levels are observed in the spectral region just above the $Z_1 \rightarrow D_4$ crystal-field transition. The polarization of all these vibronic transitions is fully consistent with their assignment (X or Z). Vibronic levels associated with the D_4 level and second harmonic vibronic levels XX and ZZ associated with the D_1 level are also identified at higher energies. Table VI summarizes the electronic and D^- local-mode energies obtained for the $^1D_2$ multiplet.

2. *Fluorescence spectra of the C_{4v} hydrogenic centers in CaF$_2$*

The polarized emission from the $^1D_2$ multiplet was recorded for selective excitation of the D_1 level, but the results are less complete than for SrF$_2$ because fewer lines appear. Representative spectra are presented in Figs. 5 and 6. The energies of the electronic levels and the local mode phonons are included in Tables V and VII, together with the transition polarizations (σ or π) from D_1. The energies of the Z_2 and Z_7 levels of the $^3H_4$ multiplet were inferred through observation of their associated (X,Y) vibronic transitions, having the expected $x(yy)z:x(yx)z$ polarization ratio of 2:1.

The Sm^{2+} emission envelope[11] centered at 14 114 cm^{-1} dominates the $^1D_2 \rightarrow {}^3H_5$ spectrum in some of the crystals and obscures many local-mode vibronic transitions. Because the Sm^{2+} absorption is broad in the region of excitation, changing the laser frequency does not improve the hydrogenic center discrimination. Time resolution, however, could be used to distinguish between the Pr^{3+} and Sm^{2+} emission in CaF$_2$ through the difference in fluorescence lifetimes.

The position of the X_3 level of the $^3H_6$ multiplet is made uncertain by the presence of a lattice phonon band associated with the X_1 electronic level. The X_3 level has been assigned to the strongest line within this band, but another component may be the correct one.

The position of the X_8 crystal-field level of the $^3H_6$ multiplet is anomalous in not following the expected isotopic trend from H^- to T^-. For the C_{4v} D^- center, its energy is out of sequence, probably as a result of the influence of the nearby (X,Y) vibronic level associated with the X_1 level.

V. ELECTRONIC ZEEMAN EFFECT

The doubly degenerate ground-state ($^3H_4,\Gamma_5^+,\gamma_5$) of a Pr^{3+} ion in a C_{4v} center has a linear Zeeman effect with a splitting factor $g_{\parallel}\beta/h$ reported to be 2.72 MHz/G for the F^- center in CaF$_2$.[8,9] In addition, there is a first-order hyperfine interaction between the Pr^{3+} $I=\frac{5}{2}$ nuclear spin and the Pr^{3+} electronic moment. Because of the large hyperfine splitting of 2.8 GHz and the small inhomogeneous linewidths, the six hyperfine lines are resolved in an excitation spectrum. Figure 7 shows the excitation line profile for the C_{4v} centers studied, as recorded in the crystal after deuteration to ensure an identical host crystal environment for both the F^- and D^- centers. The extra depth of the central minima in Figs. 7(c) and 7(d) provides further evidence of a ground-state splitting and departure from strictly C_{4v} symmetry.

The Zeeman splittings were measured for the C_{4v} D^- and F^- centers in both CaF$_2$ and SrF$_2$ by scanning a single mode dye laser and monitoring the emission to crystal-field levels of the $^3H_4$ multiplet. The results obtained for the C_{4v} D^- centers are shown in Fig. 8 and summarized in Table VIII for all the C_{4v} centers. Also listed are the first-order hyperfine splittings for the C_{4v} centers measured.

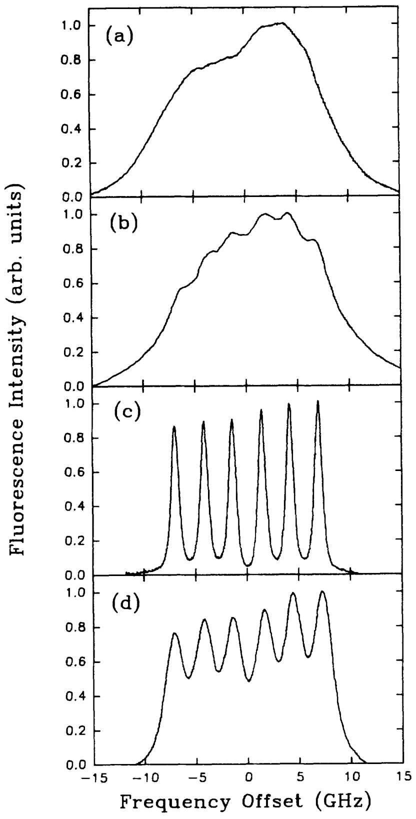

FIG. 7. 4.2 K excitation line profiles of the D_1 level for (a) the C_{4v} F^- center and (b) the C_{4v} D^- center in deuterated SrF_2:Pr^{3+}; (c) the C_{4v} F^- center and (d) the C_{4v} D^- center in deuterated CaF_2:0.01% Pr^{3+}.

The electronic g values and, consequently, the first-order hyperfine splittings both increase in going from the F^- to the D^- variety of the C_{4v} centers. There is also an increase in the inhomogeneous linewidth with D^- ions instead of F^- ions in the interstitial position.

VI. FLUORESCENCE LIFETIMES AND NONRADIATIVE DECAY FOR C_{4v} CENTERS

The fluorescence lifetimes of the ${}^1D_2$ and ${}^3P_0$ emitting levels, measured for all C_{4v} centers in CaF_2 and SrF_2, including the hydrogenic varieties, along with the energy separations between levels and the minimum number of appropriate hydrogenic ion local-mode phonons required to bridge the energy gap to the next lower multiplet, have already been reported.[6] For the purpose of discussion here the relevant lifetimes are presented in Table IX.

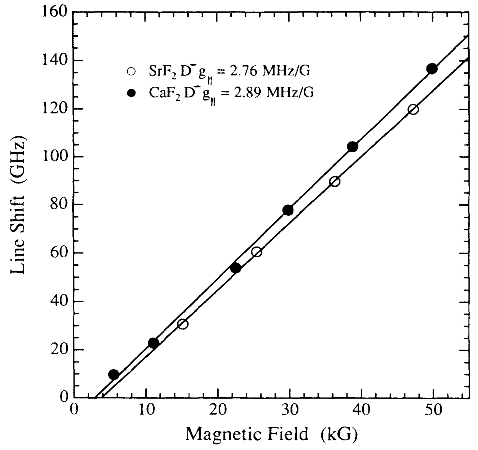

FIG. 8. Measured Zeeman shifts of the upper component of the electronic ground state of Pr^{3+} in the C_{4v} D^- center in deuterated CaF_2:Pr^{3+} and SrF_2:Pr^{3+} crystals.

A noteworthy feature of these results is the large variation of the fluorescence lifetimes with the hydrogenic ion species present. As the electronic transitions being excited in varieties of the same C_{4v} center are closely similar in symmetry and wave-function composition, radiative lifetimes can vary at most by an order of magnitude. The strong isotope dependence can, therefore, be accounted for only by nonradiative processes involving the respective local-mode phonons. Some preliminary understanding of the variation in the lifetimes was obtained with a model of multiphonon processes, involving just a single phonon frequency, bridging the energy gap to the next lower multiplet.[18] Such a model was reasonably successful in accounting for the observed lifetime variations in a phenomenological way, but a more detailed understanding would require specific considerations of the coupling between the electronic states and local-mode phonons involved in the nonradiative decay processes.

The increased probability of nonradiative relaxation processes in C_{4v} hydrogenic centers manifests itself in the presence of emission from both the ${}^3P_0$ and ${}^1D_2$ multiplets for excitation of the ${}^3P_0$ level. The strong quenching of the ${}^3P_0$ emission by the local-mode phonons efficiently feeds the ${}^3P_0$ excitation to the lower ${}^1D_2$ multiplet. This effect is only weakly present in the corresponding C_{4v} F^- center where the ${}^3P_0$ decay is largely radiative. The cascading of the ${}^3P_0$ excitation to the lower ${}^1D_2$ multiplet can be observed as a rise time of the fluores-

TABLE VIII. Electronic ground state (Z_1) $g_{\parallel}$ values (MHz/G) and hyperfine splittings (GHz) determined for Pr^{3+} ions in various C_{4v} centers in CaF_2 and SrF_2.

	CaF_2:Pr^{3+}		SrF_2:Pr^{3+}	
	C_{4v} F^- center	C_{4v} D^- center	C_{4v} F^- center	C_{4v} D^- center
Electronic g value	2.72	2.89	2.69	2.76
Hyperfine splitting	2.78	2.82	<2	2.2

TABLE IX. 10 K fluorescence lifetimes (in μs) for transitions from the $^1D_2$ and $^3P_0$ multiplets of C_{4v} centers in CaF_2:Pr^{3+} and SrF:Pr^{3+} crystals

Upper multiplet	CaF$_2$ $^3P_0$	CaF$_2$ $^1D_2$	SrF$_2$ $^3P_0$	SrF$_2$ $^1D_2$
F^-	120±5	420±10	118±5	2030±50
H^-		0.38±0.02	0.82±0.05	2.69±0.05
D^-	0.27±0.01	95±3	1.08±0.05	405±10

cence from the $^1D_2$ multiplet of about 1 μs for the C_{4v} D^- center in SrF_2. Since, as has been pointed out in Sec. IV A 2, the deexcitation from $^3P_0$ to $^1D_2$ is essentially nonradiative, the rise time of $^1D_2$ emission gives the nonradiative relaxation rate of the $^3P_0$ level,[19] and has been used in some cases to calculate nonradiative probabilities.[20]

VII. UPCONVERSION FLUORESCENCE IN THE C_{4v} CENTERS

At a 4000-fold increase in sensitivity over that used for recording fluorescence from the $^1D_2$ multiplet, fluorescence is observed from the $^3P_0$ level of C_{4v} F^- centers when the laser is tuned to pump the $^1D_2$ multiplet, i.e., upconversion emission is observed. Such upconversion has been reported[3,21] for the C_{4v} F^- center in CaF_2:Pr^{3+} and SrF_2:Pr^{3+} crystals, and it is also seen here for the C_{4v} D^- centers in SrF_2:Pr^{3+} crystals. In all cases, excitation of the $^1D_2$ multiplet of the Pr^{3+} ion yields fluorescence from the $^3P_0$ level of the same center.

Upconversion emission from the $^3P_0$ level has been observed for temperatures of up to 60 K, for the C_{4v} F^- centers of both CaF_2 and SrF_2. For the C_{4v} centers in SrF_2:Pr^{3+}, the relative upconversion emission intensities, for similar excitation conditions, are factors of 5×10^{-3}, 1×10^{-5}, and 3×10^{-6} down on the direct emission for the F^-, T^-, and D^- centers, respectively. These give order of magnitude values for the relative efficiency of upconversion in all three centers. No upconversion was observed for the H^- center at a sensitivity level 10^7 more than for the direct $^1D_2 \rightarrow {}^3H_4$ emission. The upconversion in CaF_2:Pr^{3+} is weaker than for SrF_2:Pr^{3+} and the only upconversion apparent is for the F^- center where the upconversion emission is 4×10^{-4} less than the direct.

There have been comprehensive reviews of the various possible energy transfer mechanisms[22] and more recent studies discuss processes ranging from energy transfer between triads of ions giving ultraviolet fluorescence[23] to transfer amongst ions distributed across an inhomogeneously broadened line after irradiation with a single mode laser.[24] Energy transfer phenomena can be broadly classified as either ion pair relaxation or upconversion. Ion pair relaxation occurs when an excited donor ion relaxes by transferring all or part of its energy to an initially unexcited acceptor ion. If two ions are initially excited, however, one can decay by transferring its energy to the other which then has an energy greater than its initial excitation energy. It is this latter process that leads to upconversion which is of interest here.

Since the accepted model of the C_{4v} centers is of isolated single rare-earth ions and their single charge compensator ions, it was at first expected that upconversion would occur from a sequential two-photon excitation process,[25] often referred to as the STEP mechanism. However, the upconversion results to be described are consistent with the alternative energy transfer upconversion (or ETU) process[26] involving energy transfer between two Pr^{3+} ions of a pair of C_{4v} centers in close proximity, i.e., a subset of the ensemble of C_{4v} centers.

Polarized $^3P_0$ emission for the C_{4v} F^- center in SrF_2 was recorded for both direct excitation (using the argon ion laser) [Fig. 4(b)] and for upconversion excitation from the $^1D_2$ multiplet. Identical polarization spectra are observed for either direct of upconversion excitation. The polarization is determined by the selection rule for the absorption transition ($\gamma_5 \rightarrow \gamma_{a'}$) which is the same for either $^1D_2$ or $^3P_0$ excitation. Either the same Pr^{3+} ion absorbs both photons for that polarization geometry sequentially in a STEP mechanism or two identical excited Pr^{3+} ions combine their excitation to give upconversion in an ETU process.

It is unlikely that the $^1D_2$ level could be the sole intermediate level in a STEP mechanism as no energy levels are expected at twice the photon frequency. Invoking an intermediate decay to, for example, the $^3H_6$ multiplet before absorption of the second photon gives a better energy match for reaching the $^3P_0$ level.[27]. In this case there would be a time delay between absorption of the first and second photons. Observation of the upconversion under pulsed excitation conditions discounts the STEP mechanism, as there is insufficient time during the period of the laser pulse (1 ns) for the ion to relax to the intermediate $^3H_6$ state before absorbing a second photon. Another observation is that maximum upconversion fluorescence intensity is reached for a $^1D_2$ excitation energy about 0.25 cm^{-1} lower than that required to give the strongest direct fluorescence. This is consistent with the model of weakly interacting pairs of C_{4v} centers[3] in which a specific subset of the C_{4v} centers, with slightly shifted energy levels from the isolated C_{4v} centers, participate in upconversion.

A two-laser experiment verified this model of ETU upconversion. With a cw laser tuned for maximum upconversion emission from the C_{4v} F^- center in SrF_2, a second laser, having its beam exactly coincident with that of the first laser through the crystal, produced extra upconversion only when its frequency matched that of the first laser. No intermediate level, with energy differing from the $^1D_2$ level, appears to be involved.

The ETU upconversion mechanism proposed for Pr^{3+} differs from the case of Nd^{3+} where there is clear evidence of STEP upconversion.[28] For Nd^{3+} a cw laser tuned to the ${}^4F_{3/2} \rightarrow {}^4D_{3/2}$ interval of 16 515 cm^{-1} for the C_{4v} F^- center in CaF_2:Nd^{3+} gave upconversion to the ${}^4D_{3/2}$ level at 28 109 cm^{-1} through a second photon being absorbed by the excited state ${}^4F_{3/2}$ level at 11 594 cm^{-1}, which was itself being populated from the ground state via a phonon sideband of the ${}^2H_{11/2}$ level. Nevertheless, this STEP mechanism is quite weak and would be enhanced by direct excitation of the ${}^4F_{3/2}$ level by a suitably tuned second laser. The observation of this STEP mechanism does not preclude the simultaneous presence of ETU processes for nearby Nd^{3+} C_{4v} F^- centers.

The observation of upconversion under pulsed excitation allows the concentration dependence of the upconversion lifetimes to be studied. The fluorescence lifetime of the upconverted emission from the ${}^3P_0$ level of the C_{4v} F^- center in SrF_2 was measured for Pr^{3+} ion concentrations of 0.05, 0.1, and 0.5%, as 550±50, 470±20, and 220±20 μs, respectively. The upconversion is both more intense and has shorter lifetime for increased Pr^{3+} concentration. The temporal behavior of the upconversion process involving ion pairs has two regimes depending on whether the transfer rate of excitation between the ions is large or small.[29] If the rate is small, the decay has half the lifetime of the ${}^1D_2$ level; if it is large the rise time of the upconverted emission is of the order of the inverse of the transfer rate while the decay time is the same as that of the ${}^3P_0$ level. Evidence for these two regimes is provided by the concentration dependence of the decay of the upconverted ${}^3P_0$ emission measured here. At a low Pr^{3+} concentration, the average separation of centers is large and the upconversion is primarily by those centers having a small transfer rate. The 550 μs lifetime measured for the 0.05% crystal is approaching the limiting value of 1 ms set by half the ${}^1D_2$ lifetime. In the higher concentration crystals the average intercenter separation shortens and the upconversion has a large contribution from the closer ion pairs. Here the decay of the upconversion emission is set by the ${}^3P_0$ lifetime at 118 μs. Some discussion of the transfer rate mechanisms in the case of the C_{4v} F^- center in CaF_2:Pr^{3+} suggests a rate varying as the inverse sixth power of the interionic separation R, consistent with electric dipole-dipole coupling.[3]

The variation of the relative upconversion efficiencies for different varieties of the C_{4v} centers can be understood through the variation of the fluorescence lifetime of the ${}^1D_2$ level for those centers. The number of Pr^{3+} ions excited to the higher energy ${}^3P_0$ state depends on the number of ion pairs able to participate and this is set by the time a Pr^{3+} ion remains in the ${}^1D_2$ state. If the transfer rate is slower than the ${}^1D_2$ decay rate then there will be fewer pairs available to participate in the upconversion and the upconversion efficiency will fall. This qualitatively accounts for the weaker upconversion for C_{4v} F^- centers in CaF_2 compared to SrF_2 since the relevant ${}^1D_2$ lifetimes decrease from 2.03 ms in SrF_2 to 420 μs in CaF_2. A similar situation occurs for the relative upconversion efficiencies of the C_{4v} D^-, T^-, and F^- centers in SrF_2; the change in respective lifetimes is the principal factor governing the process, with the relative concentration of the appropriate centers also determining the level of upconversion emission efficiency observed.

VIII. CONCLUSIONS

The comprehensive sets of energy levels established for the various varieties of the C_{4v} centers of Pr^{3+} ions in SrF_2 and CaF_2 provide a basis both for crystal-field calculations, where the effect of the differing charge compensating ions can be examined, and calculations of the vibronic splittings apparent in the doubly degenerate (X,Y) local-mode transition observed in either infrared absorption or in the local-mode vibronic fluorescence of the Pr^{3+} ion.

The marked variation in the fluorescence lifetimes between the various C_{4v} centers provides data for investigation of nonradiative decay processes involving the respective local-mode phonons through the electron-local-mode phonon interaction.

ACKNOWLEDGMENTS

This research was supported by the New Zealand University Grants Committee and the New Zealand Lottery Board through Research Grants. We wish to thank Dr. C. A. Freeth of the University of Wollongong for involvement in some fluorescence lifetime and upconversion spectra measurements carried out at the Australian National University and Dr. R. M. Macfarlane for help with the Zeeman measurements carried out at the IBM Almaden Research Center, San Jose, California. We also acknowledge technical assistance from R. A. Ritchie, T. Rowe, and W. G. Smith.

---

*Present address: University Center for Laser Research, Oklahoma State University, Stillwater, Oklahoma 74078-0444.

[1] N. J. Cockroft, D. Thompson, G. D. Jones and R. W. G. Syme, J. Chem. Phys. **86**, 521 (1987).

[2] J. L. Sommerdijk, A. Bril, and A. W. de Jager, J. Lumin. **9**, 288 (1974); V. P. Bhola, Phys. Status Solidi **68**, 667 (1975); V. P. Bhola, J. Lumin. **10**, 185 (1975); J. Duran and M. Billardon, J. Phys. C **5**, 3110 (1972); J. Kliava, P. Evesque, and J. Duran, *ibid.* **11**, 3357 (1978); R. H. Petit, P. Evesque, and J. Duran, *ibid.* **14**, 5081 (1981); P. Evesque, J. Kliava, and J. Duran, J. Lumin. **18/19**, 646 (1979); John Chrysochoos, *ibid.* **31/32**, 172 (1984); J. Chrysochoos, P. W. M. Jacobs, M. V. Stillman, and A. V. Chadwick, *ibid.* **128**, 179 (1983); Brian M. Tissue and John C. Wright, Phys. Rev. B **36**, 9781 (1987); J. Lumin. **44**, 33 (1989).

[3] Arturo Lezama, Marcos Oria, and Cid B. de Araujo, Phys. Rev. B **33**, 4493 (1986).

[4] R. W. G. Syme, R. J. Reeves, and G. D. Jones, J. Lumin. **31/32**, 248 (1984).

[5] R. J. Reeves, G. D. Jones, and R. W. G. Syme, Phys. Rev. B **40**, 6475 (1989).

[6] R. J. Reeves, G. D. Jones, N. J. Cockroft, T. P. J. Han, and R.

W. G. Syme, J. Lumin. **38**, 198 (1987).

[7] J. L. Hall and R. T. Schumacher, Phys. Rev. **127**, 1892 (1962).

[8] R. M. Macfarlane, R. M. Shelby, and D. P. Burum, Optics Lett. **6**, 593 (1981); D. P. Burum, R. M. Shelby, and R. M. Macfarlane, Phys. Rev. B **25**, 3009 (1982).

[9] R. M. Macfarlane, D. P. Burum, and R. M. Shelby, Phys. Rev. B **29**, 2390 (1984).

[10] I. T. Jacobs, Ph.D. thesis University of Canterbury, New Zealand, 1971 (unpublished).

[11] D. L. Wood and W. Kaiser, Phys. Rev. **126**, 2079 (1962).

[12] Yu.K. Voron'ko, A. A. Kaminskii, and V. V. Osiko, Zh. Eksp. Teor. Fiz. **49**, 420 (1965) [Sov. Phys. JETP **22**, 295 (1966)]; A. Edgar, C. A. Freeth, and G. D. Jones, J. Phys. C **15**, 6833 (1982).

[13] G. D. Jones, S. Peled, S. Rosenwaks, and S. Yatsiv, Phys. Rev. **183**, 353 (1969); A. Edgar, C. A. Freeth, and G. D. Jones, Phys. Rev. B **15**, 5023 (1977).

[14] A. Edgar, G. D. Jones, and M. R. Presland, J. Phys. C **12**, 1596 (1979).

[15] B. G. Wybourne, *Spectroscopic Properties of Rare Earths* (Interscience, New York, 1965).

[16] Y. L. Khong (private communication).

[17] I. T. Jacobs, G. D. Jones, K. Zdansky, and R. A. Satten, Phys. Rev. B **3**, 2888 (1971).

[18] L. A. Riseberg and H. W. Moos, Phys. Rev. Lett. **19**, 1423 (1967); Phys. Rev. **174**, 429 (1968).

[19] Yu. E. Perlin and A. A. Kaminskii, Phys. Status Solidi **B132**, 11 (1985).

[20] T. Kushida and J. E. Geusic, Phys. Rev. Lett. **21**, 1172 (1968).

[21] G. D. Jones, N. J. Cockroft, T. P. J. Han, R. J. Reeves, and R. W. G. Syme, in *Proceedings of the Second Asia Pacific Conference,* edited by S. Chanrasekhar (World Scientific, Singapore, 1987), pp. 648-655.

[22] J. C. Wright, in *Topics in Applied Physics Vol. 15* (Springer Verlag, Berlin, 1976), pp. 239–295; L. A. Riseberg and M. J. Weber, in *Progress in Optics XIV,* edited E. Wolf (North Holland, Amsterdam, 1976), pp. 89–153.

[23] A. Lezama, M. Oria, J. R. Roos Liete, and C. B. De Araujo, Phys. Rev. B **32**, 7139 (1985).

[24] R. Flach, D. S. Hamilton, P. M. Selzer, and Y. M. Yen, Phys. Rev. Lett. **35**, 1034 (1975).

[25] N. Bloembergen, Phys. Rev. Lett. **2**, 84 (1959).

[26] T. Miyakawa and D. L. Dexter, Phys. Rev. **B1**, 70 (1970).

[27] G. H. Dieke, *Spectra and Energy Levels of Rare Earth Ions in Crystals* (Interscience, New York, 1968), p. 142.

[28] T. P. J. Han, PhD. thesis, University of Canterbury, New Zealand, 1989 (unpublished).

[29] R. Buisson and J. C. Vial, J. Phys. Lett. (Paris) **42**, L115 (1981).